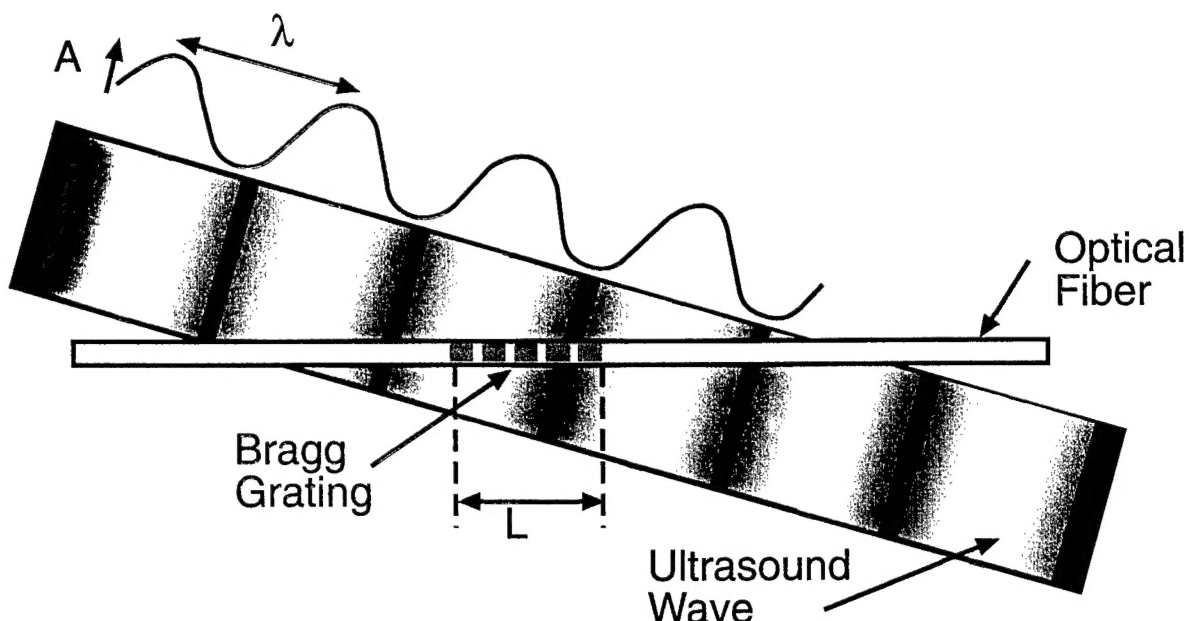


A Technology Assessment of

# Bragg Grating Fiber Optic Based Nondestructive Evaluation (NDE)

NTIAC-TA-01-02



*Interaction of Ultrasound Wave with Light Wave Going Through a Fiber Bragg Grating*

**DISTRIBUTION STATEMENT A**

Approved for Public Release  
Distribution Unlimited

20020124 400

**NTIAC**

Nondestructive Testing Information Analysis Center  
A DoD Information Analysis Center Sponsored by the  
Defense Technical Information Center (DTIC)

September 2001

This document was prepared by the Nondestructive Testing Information Analysis Center (NTIAC), TRI/Austin, Inc., 415 Crystal Creek Drive, Austin, TX 78746-4725. NTIAC is a full service information analysis center operated under Contract SPO700-97-D-4003 for the U.S. Department of Defense, serving the information needs of the Department of Defense, other U.S. Government agencies, and the private sector in the field of nondestructive testing.

NTIAC is sponsored by the Defense Technical Information Center (DTIC) and administered by the Defense Information Systems Agency (DISA). Technical aspects of NTIAC operations are monitored by the Office of the Deputy Undersecretary of Defense (S&T).

Additional copies of this document may be obtained from:

NTIAC  
415 Crystal Creek Drive  
Austin, TX 78746-4725  
Phone: (512) 263-2106 or (800) NTIAC 39  
Fax: (512) 263-3530  
E-mail: info@ntiac.com

ISBN 1-890596-21-3

This document was prepared under the sponsorship of the U.S. Department of Defense. Neither the United States Government nor any person acting on behalf of the United States Government assumes any liability resulting from the use or publication of the information contained in this document or warrants that such use or publication of the information contained in this document will be free from privately owned rights.

Use of trade names of manufacturers in this publication does not constitute an official endorsement of such products or manufacturers, either expressed or implied by the Department of Defense or NTIAC.

Approved for public release; distribution unlimited

All rights reserved. This document, or parts thereof, may not be reproduced in any form without written permission of the Nondestructive Testing Information Analysis Center.

Copyright<sup>©</sup> 2001, Nondestructive Testing Information Analysis Center.

Cover Acknowledgement: Perez, I. M., H. L. Cui, E. Udd, "High Frequency Ultrasonic Wave Detection Using Fiber Bragg Gratings," *SPIE Smart Structures Conference*, March, 2000, Bellingham, Washington: The International Society for Optical Engineering (SPIE).

A Technology Assessment of  
**Bragg Grating Fiber Optic Based  
Nondestructive Evaluation (NDE)**

*By*

H. Thomas Yolken

*And*

George A. Matzkanin



Nondestructive Testing Information Analysis Center  
A DTIC-Sponsored DoD Information Analysis Center  
Operated by TRI/Austin, Inc., *A Texas Research International Company*

September 2001

Approved for Public Release; Distribution Unlimited

## **Preface**

This Critical Review was prepared under NTIAC Contract No. SOI700-97-D-4003 which is funded by the Defense Technical Information Center (DTIC).



## CONTENTS

	Page
Preface.....	iii
List of Figures.....	vii
List of Tables.....	xi
1.0 INTRODUCTION.....	1
2.0 TECHNOLOGY DESCRIPTION .....	3
3.0 REVIEW OF REPORTED APPLICATIONS .....	13
3.1 Determination of Temperature and Strain .....	13
3.2 Composite Processing .....	20
3.3 Monitoring of Civil Structures.....	24
3.4 Chemical Sensor .....	33
3.5 Corrosion .....	33
3.6 Adhesive Joints .....	35
3.7 Acoustic Emission and Ultrasonic Waves .....	38
4.0 CONCLUSIONS AND PROGNOSIS .....	41
4.1 Conclusions and Summary .....	41
4.2 Prognosis/Recommendations .....	42
5 REFERENCES.....	43
6 BIBLIOGRAPHY.....	47



## List of Figures

	Page
Figure 2-1	Twin core sensor principle .....4
Figure 2-2	Formation of a Bragg grating in a optical fiber .....4
Figure 2-3	Diagram of the experimental setup for transverse holography method .....5
Figure 2-4	Illustration showing fiber grating reflector and the Bragg condition for reflection .....6
Figure 2-5	Wavelength division multiplexing of fiber grating sensors using broadband sources .....7
Figure 2-6	Arrangement for fabricating fiber Bragg grating filters and taps by the side-writing technique. The inset is a schematic of a Bragg grating tap in a D-shaped elliptical core fiber .....7
Figure 2-7	Schematic of a fiber Bragg grating tap which is blazed to radiate a beam at an angle $\gamma_B$ measured from a normal to the cladding-air interface .....8
Figure 2-8	Schematic of photographic apparatus for photoimprinting a refractive index Bragg grating in a photosensitive optical fiber waveguide .....9
Figure 2-9	Schematic diagram of the excimer laser interferometer used to write the gratings during the fiber draw .....10
Figure 2-10	Fracture stress versus stress rate and 50%-quantile fits for pristine fiber A at 21°C (filled symbols) and 230°C (open symbols) .....12
Figure 3-1	Contributing factors to temperature and strain sensitivity..... 13
Figure 3-2	Technique for quasi-distributed strain sensing using in-fiber Bragg gratings .....14
Figure 3-3	Fiber optic Bragg grating based differential sensor system .....15

Figure 3-4	Phase difference output recorded over a 30 min period for various differential temperatures applied to the gratings .....	16
Figure 3-5	Schematic of the fiber laser strain sensor system .....	16
Figure 3-6	Fiber laser output wavelength as a function of strain on the Bragg grating .....	17
Figure 3-7	Diagram of strain sensor configuration using a fibre Bragg grating and wavelength division coupler .....	18
Figure 3-8	Response of sensor output voltage to three-point bending induced strain .....	19
Figure 3-9	Extrinsic Fabry-Perot interferometer for the measurement of strain .....	20
Figure 3-10	Bragg grating fiber optic sensor for measurement of strain .....	21
Figure 3-11	Output of Bragg grating sensor during cure corrected for thermal apparent strain .....	21
Figure 3-12	Process induced strains measured with the extrinsic Fabry-Perot interferometers .....	22
Figure 3-13	Comparison of output from Bragg grating sensor during normal and dry pultrusion .....	23
Figure 3-14	Experimental setup for mechanical testing of pultruded Tendons .....	24
Figure 3-15	Strain vs. time plot from extensometer and embedded Bragg grating sensor in a glass composite tendon subjected to a sinusoidal load .....	24
Figure 3-16	Moment ratio vs. tensile strain on fiber optic Bragg grating sensor embedded in a large scale T-shaped concrete beam .....	25
Figure 3-17	Average crack-width measurement obtained from fiber optic Bragg grating sensors and micrometer .....	26
Figure 3-18	Optical measurement system fiber optic Bragg grating sensor for strain measurement .....	27
Figure 3-19	Typical wavelength shift as a result of strain on fiber optic Bragg grating sensor .....	27

Figure 3-20	Schematic diagram of the 60 channel fiber Bragg Grating (FBG) sensor electro-optics system for monitoring strain in bridges .....	28
Figure 3-21	Schematic diagram for the dynamic fiber Bragg grating (FBG) bridge interrogation system .....	29
Figure 3-22	Schematic of bridge section .....	30
Figure 3-23	Fiber Bragg grating sensor placement in concrete deck .....	30
Figure 3-24	Fiber Bragg grating sensor placement under steel I-beams .....	30
Figure 3-25	Sensor placement in concrete cylinders .....	31
Figure 3-26	Comparison of axial strain gage results from concrete Cylinders .....	32
Figure 3-27	Comparison of hoop strain gage results from concrete Cylinders .....	32
Figure 3-28	Schematic of a multi-point fiber Bragg grating chemical sensor system .....	33
Figure 3-29	Absorption spectral of Ferroin .....	34
Figure 3-30	Potential concept for a Tapped Bragg Grating corrosion Sensor .....	35
Figure 3-31	Axial and transverse load sensing directions of multi-axis fiber grating strain sensor .....	36
Figure 3-32	Response of multi-axis fiber grating strain sensor to axial and transverse strains .....	36
Figure 3-33	Multi-axis strain sensors embedded into inner (left) and edge (right) locations of adhesive bond with different orientations .....	36
Figure 3-34	Retrofit of multi-axis sensor to existing adhesive joint .....	37
Figure 3-35	Loading and demodulation setup during tensile testing of instrumented adhesive joints .....	37
Figure 3-36	Block diagram of the experimental setup for characterizing Bragg grating sensors .....	39

Figure 3-37	Pulse acoustic signal, trigger, and response at 355 kHz .....	39
Figure 3-38	Response of fiber Bragg grating sensor to acoustic emission as a function of frequencies .....	40
Figure 3-39	Schematics of interaction of ultrasound wave with light wave going through a fiber Bragg grating .....	40

## **List of Tables**

	Page
Table 2-1 Environmental operation conditions for polyimide re-coated fiber optic Bragg grating .....	11

## **1.0 INTRODUCTION**

Fiber optic sensor technology has advanced considerably in the last two decades and has found many applications in science and engineering. Among other things, optical fiber sensors are well suited for measurements in harsh environments. Optical fiber based sensors offer a number of significant advantages and unique features which make them attractive for use in structural monitoring. These include the capability to sense a variety of physical parameters, the ability to profile a measurand over the length of the fiber, the ability to multiplex several measurands onto a single sensing fiber, and high compatibility for embedding in a range of structural materials.

Since the advent of photo-induced Bragg gratings in optical fibers in 1978, Bragg fiber gratings have found many applications in telecommunications and sensing. Bragg gratings have emerged as elegant in-fiber sensors particularly suitable for multiplexed and distributed applications. The growing interest and rapid progress made in the area of strain sensing using Bragg grating based sensor systems indicates recognition of the fact within the sensor community that fiber Bragg grating based sensors provide powerful sensing techniques which can be uniquely applied to a range of structural sensing applications. As a result, there has been increasing interest in using fiber Bragg grating sensors for multipoint strain monitoring within the smart structures community.

This report provides an assessment and review of the use of Bragg grating sensors for nondestructive evaluation (NDE) applications, including structural health monitoring. Section 2.0 provides a description of the physical principles underlying Bragg grating fiber optic sensors for NDE based on a chronological history of the development of Bragg grating technology. In Section 3.0 brief reviews are given of reported applications of Bragg grating sensors. The principal applications have been:

- Determination of temperature and strain
- Monitoring of composites
- Large civil structure monitoring
- Sensing for acoustic emission
- Monitoring of adhesive joints
- Chemical sensing
- Corrosion detection

Conclusions and a prognosis of Bragg grating technology for NDE are presented in Section 4.0. A list of references and a bibliography are also provided.



## 2.0 TECHNOLOGY DESCRIPTION

The physical principles underlying Bragg grating fiber optic based NDE sensors, along with fabrication approaches and characterization and reliability of the sensors is presented in this section. The small size, good sensitivity and intrinsic nature of Bragg grating fiber optic sensors make them ideal for embedded sensors in smart structures or surface monitoring applications. The output of Bragg grating sensors are inherently wavelength encoded and therefore require a scheme to detect small wavelength shifts that correspond to the detected parameter. A considerable amount of research has been directed towards developing wavelength demodulation techniques. Several techniques have been demonstrated based on using interferometric detection and fiber Fabry-Perot filters. The following papers give a chronological history of the development of Bragg grating technology including physical principles, fabrication approaches and reliability.

In a seminal paper, Hill et al. (1978) at the Communications Research Centre, Department of Communications, in Canada reported on the development of a new photosensitive mechanism in a Ge-doped silica core fiber manifested by light-induced refractive index changes. Hill et al. utilized this phenomenon to form high quality, long length, refractive filters in fibers. They fabricated tunable, high quality, optical waveguide filters with low scattering loss and potential for extremely high frequency selectivity. The filters are formed in a low mode number, silica fiber waveguide by exposure of the photosensitive core of the fiber to intense contra-directionally propagating coherent light beams. The light beams are excited in the fiber with the aid of a single mode, argon ion laser, operated on either the 488.0 or 514.5- nm line. Standing waves patterns are produced and result in the exposures to the fiber that form the periodic perturbations that comprise the filter. This photosensitive or photoinduced phenomenon demonstrated by Hill et al. was a new approach to fabricating optical fiber filters and provided the foundation for work that followed on Bragg Grating filters and sensors

Hill et al. (1978) demonstrated that these filters, with reflectivity reaching nearly 100 % of the light launched in the core, can be used as distributed feedback structures to replace the output reflector of an argon-ion laser. The researchers predicted that these filters would have many potential applications including laser mode control and as synthesized filters with tailored response characteristics for use in high capacity, wavelength-multiplexed light-wave communication systems. Hill et al. were able to demonstrate the first reported distributed feedback oscillation of a gas laser operating in the visible region of the spectrum.

In 1987, Meltz et al. developed new twin-core, polarimetric and in-fiber-grating sensors designed to measure temperature and local strain in the in-situ monitoring of polymer composites. A twin-core sensor was used as a form of differential interferometer. It consisted of a dual mode optical waveguide containing a pair of closely spaced, single mode cores in a common cladding as shown in Figure 2-1. The technique shown in Figure 2-2 was used to produce the Bragg gratings. The technique relies on the formation of a two beam interference pattern with the angles of the interfering beams (i.e., the periodicity of the interference pattern) adjusted so that the Bragg condition would be

satisfied for a wavelength of 590 nm. Meltz et al. concluded that they had produced a new means for making quasi-distributed measurements of temperature and strain by using Bragg grating sensors. The temperature and strain sensitivity of the in-fiber grating is derived from the Bragg condition which relates the wavelength of the reflected radiation at line or wavelength center  $\lambda_0$  to the grating period  $\Lambda$  as shown in equation:

$$\lambda_0 = 2 n_{\text{core}} \Lambda$$

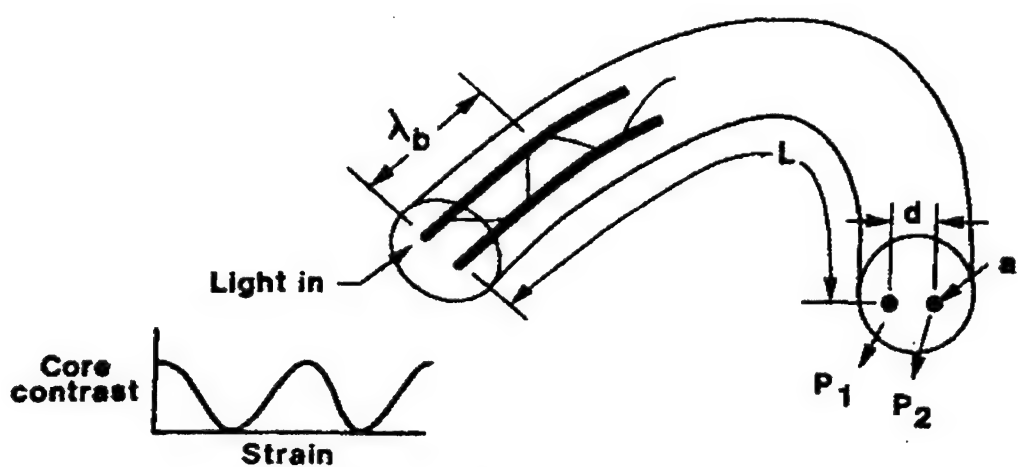


**Figure 2-1** Twin core sensor principle  
(Meltz et al, 1987)

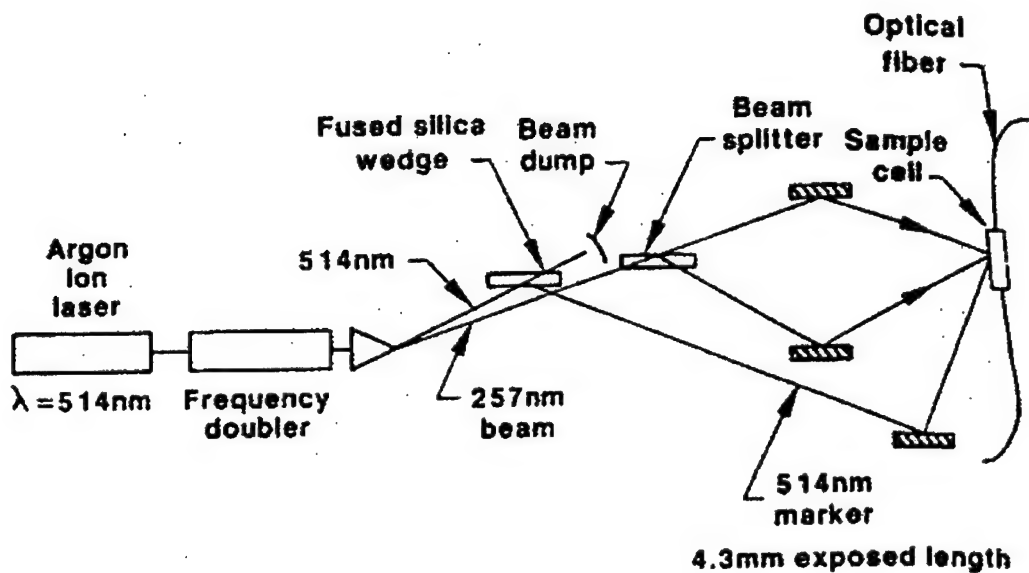


**Figure 2-2** Formation of a Bragg grating in an optical fiber  
(Meltz et al, 1987)

An important advance in Bragg grating sensor technology was made by Meltz et al. in 1989 when it was shown that in-fiber Bragg gratings can be formed by illuminating the fiber core from the side of the fiber with coherent UV radiation that lies in the 244-nm germania oxygen-vacancy defect band. This intense absorption band coincides with the second harmonic of both blue-green laser lines. The new technique was described as formation of Bragg gratings in optical fibers by a transverse holographic method. Figure 2-3 shows the experimental arrangement. A tunable excimer-pumped dye laser operated in the range of 486-500 nm with a frequency doubling crystal is used to provide a UV source with adequate coherence length. The UV radiation is split into two equal intensity beams and then recombined to produce an interference pattern within the core of the fiber. A monochromator is used to measure the reflection spectrum of the Bragg grating. This constituted an important contribution to the field because the technique expanded the range and choice of the Bragg period or spacing.

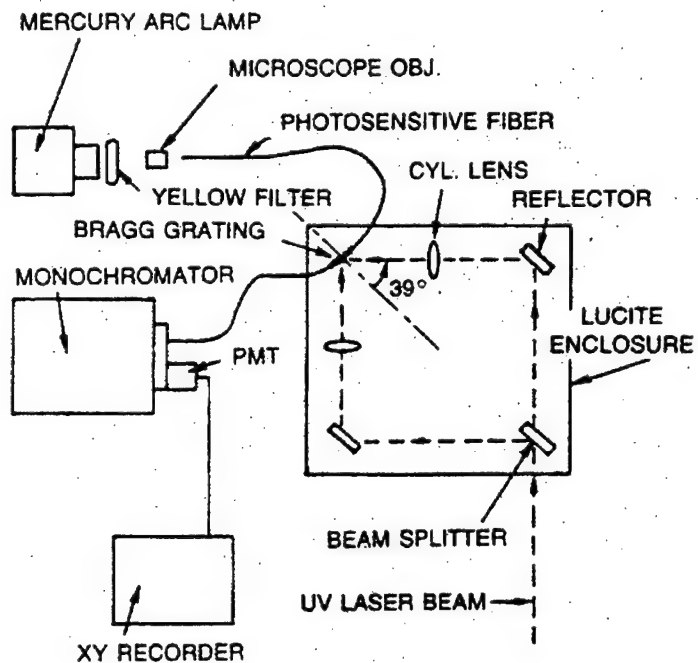


**Figure 2-3** Diagram of the experimental setup for transverse holography method  
(Meltz et al, 1989)

Continued advancements in Bragg grating research resulted in approaches for multiplexing fiber optic Bragg grating sensors (Morey et al. 1991). Figure 2-4 shows the Bragg Grating sensors constructed using a holographic writing technique on the core of commercially available commercial fibers. A period modulation of the index of refraction is produced in the germania doped core of the fiber by the interfering UV beam fringes that bleach the oxygen vacancy defect adsorption band. The authors presented a review of how Bragg grating sensors are produced and the basis of their operations including the measurement of temperature and strain. When temperature and/or strain are applied to a section of the fiber containing a grating, the grating spacing and index of refraction are modified and hence the Bragg wavelength changes. The major advantage

of a grating sensor is that it responds with a wavelength change rather than an amplitude change and great sensitivity can be obtained from detecting very small changes in wavelength.

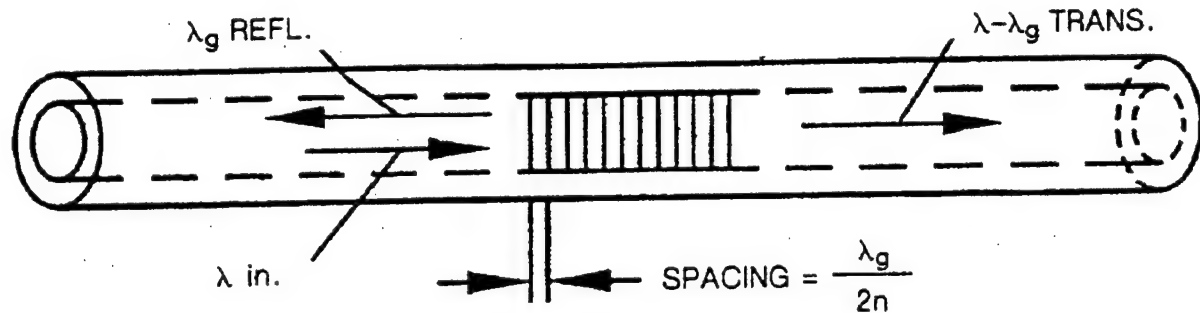


**Figure 2-4** Illustration showing fiber grating reflector and the Bragg condition for reflection  
(Morey et al, 1991)

Various multiplexing schemes can be used for multiple sensors on a single fiber optic (Morey et al. 1991). Figure 2-5 shows one of the techniques, namely, wavelength division multiplexing. In this case, two broadband edge light emitting diodes (ELED) are coupled into a single fiber with a wavelength division multiplexing (WDM) coupler. The source signals are then sent through a 3db wideband (WB) coupler and into a string of reflective fiber grating sensors. The return sensor signals are sent to a spectrum analyzer for measurement of the individual wavelengths from each sensor. For a 1% strain, a wavelength range of about 10 nm is required. Morey et al. used a commercial edge light emitting diode that can provide 50 to 100 microwatts of optical power into a single mode fiber with bandwidths over 100 nm wide. With this source bandwidth, the system shown in Figure 2-5 could measure about 20 sensor elements.

Morey and colleagues also developed and demonstrated a time division multiplexing (TDM) scheme for multiple sensors (Morey et al. 1991). With this approach over 100 sensors could be used on a single fiber to measure the same or different quantities. Morey et al. also demonstrated application to composite material cure monitoring and smart material monitoring at up to 500 degrees C. It was concluded that this high density multiplexing capability would have important applications for monitoring structures and smart structures.

A fiber optic Bragg grating tap technique was developed and demonstrated by Meltz et al. (1991). This technique provides a Bragg grating radiation coupler that will efficiently tap light out of the core. This technique allows for localized excitation and detection of fluorescent species on or near the fiber cladding. Figure 2-6 shows the instrumentation used to fabricate fiber Bragg grating filters and taps by the side writing technique. The technique uses a pair of focused intersecting, coherent UV beams to form period, permanent refractive index perturbations. Operation of this equipment is described in detail in Meltz et al. (1991). Figure 2-7 is a schematic of a fiber optic Bragg grating tap. Meltz and colleagues used this tap technique to develop a distributed fiber optic chemical

sensor. Tapped Bragg grating (TBG) sensors offer the potential for using optical excitation in a distributed sensor array that can be multiplexed by using time domain techniques and short pulses. A description of the chemical sensor applications demonstrated by the authors will be discussed in a latter section of this report on applications.

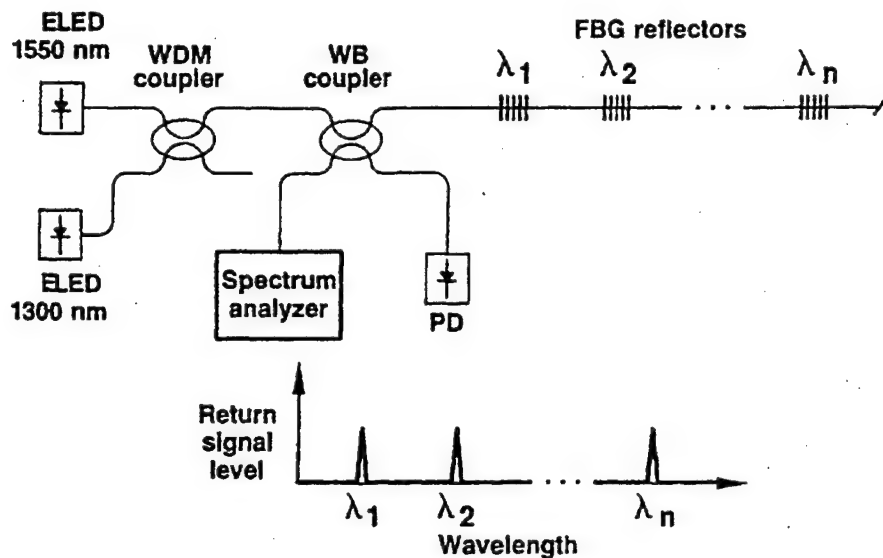


**Figure 2-5** Wavelength division multiplexing of fiber grating sensors using broadband sources  
(Morey et al, 1991)

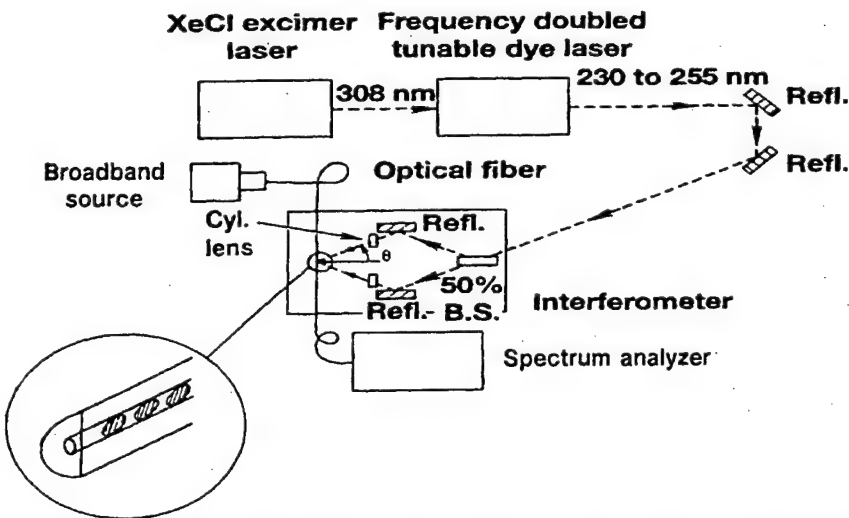


**Figure 2-6** Arrangement for fabricating fiber Bragg grating filters and taps by the side-writing technique. The inset is a schematic of a Bragg grating tap in a D-shaped elliptical core fiber  
(Meltz et al, 1991)

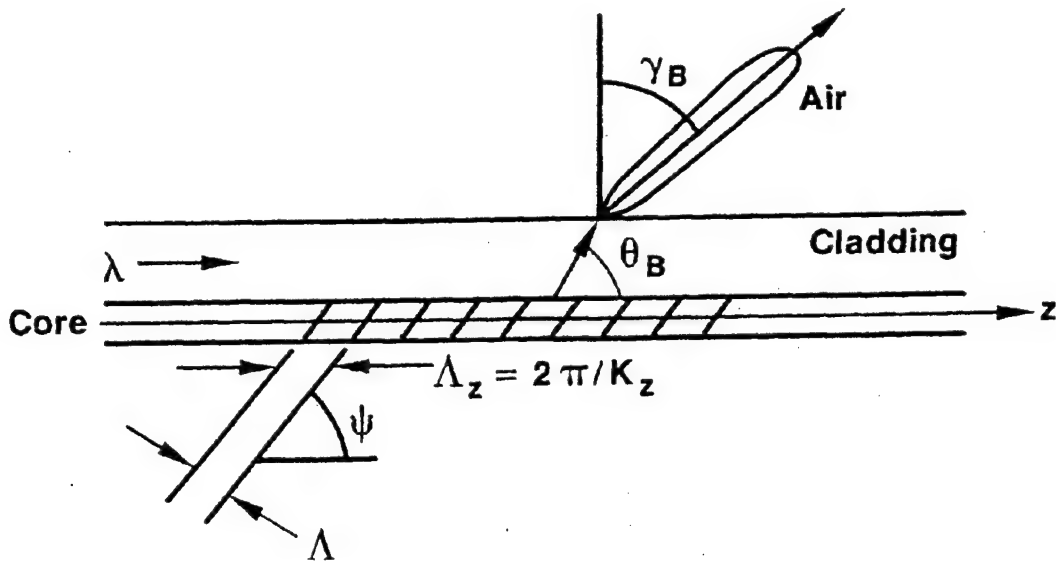


**Figure 2-7** Schematic of a fiber Bragg grating tap which is blazed to radiate a beam at an angle  $\gamma_B$  measured from a normal to the cladding-air interface  
 (Meltz et al, 1991)

Bragg gratings can also be fabricated by exposing monomode photosensitive optical fibers to UV exposure through a phase mask (Hill et al. 1993). Figure 2-8 is a schematic of the apparatus used for photoimprinting a Bragg grating in a photosensitive optical fiber waveguide. Hill et al. concluded that computer controlled, photolithography imprinting through a phase mask offers great flexibility for varying the pitch and the strength of the Bragg grating coupling coefficients. In addition, they believed that the methodology could yield high-performance, low-cost devices.

The use of optical low-coherence reflectometry to characterize Bragg gratings has been demonstrated by Lambelet et al. (1993). Optical low-coherence reflectometry is an interferometry technique that was developed in 1987 to characterize the position of weakly reflecting defects in optical waveguide elements. Lambelet et al. used an approach which incorporates a Michelson interferometer with a broad band light source, e.g., an LED. It was concluded that optical low-coherence reflectrometry can be used as an NDE technique to evaluate the position, the length, and the index modulation of the Bragg grating.

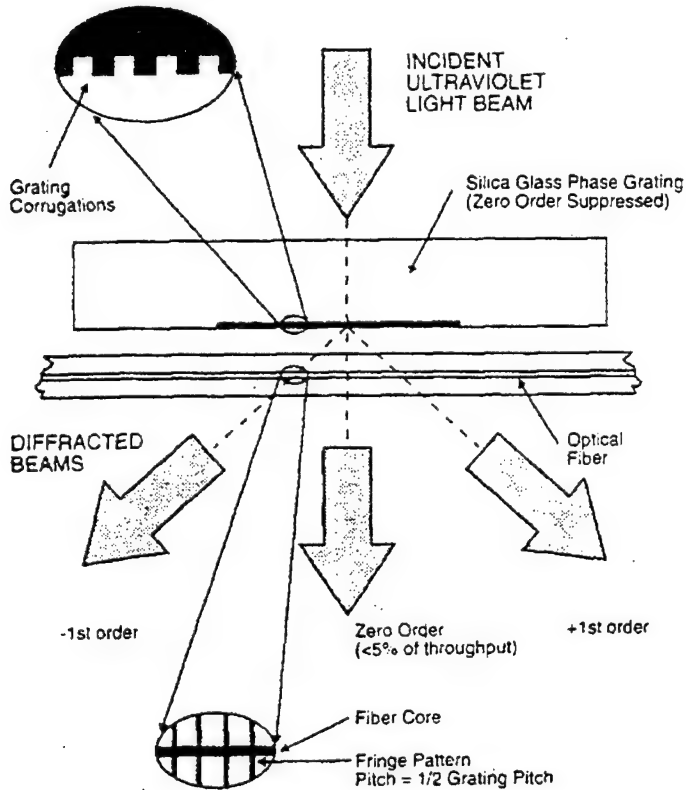


**Figure 2-8** Schematic of photographic apparatus for photoimprinting a refractive index Bragg grating in a photosensitive optical fiber waveguide  
(Hill et al, 1993)

A new in-line technique for making Bragg grating fiber optic sensors was developed by Askins et al. (1994). This new fabrication technique was viewed as having three advantages over earlier techniques. Firstly, more than 450 fiber Bragg grating sensors could be fabricated in a period of one hour as the fibers were being drawn in the manufacturing process. This is in contrast to earlier off-line efforts where only several Bragg grating sensors could be produced per day. Askins et al. used single pulses of a KrF excimer laser. Secondly, this fabrication technique allows the writing to take place before application of the protective polymer coating thus assuring a pristine surface condition. Thirdly, and perhaps the most importantly, Askins and colleagues demonstrated that arrays of grating on a single fiber could be written at different Bragg wavelengths by using an automated, computer controlled interferometer. The capability to write at a number of different Bragg wavelengths gives a huge advantage because it provides the capability to serial multiplex the sensors on a single fiber. This was in contrast to earlier work where the on-line fabrication of gratings was limited to a single wavelength (Dong et al. 1993).

Figure 2-9 is a schematic of the apparatus Askins et al (1994) used to write the Bragg gratings on a fiber as it was being drawn and before the coating process. The authors explained in detail the light path of their optics including mirrors M1, M2, M3 and M4,

the beam splitter BS, and the focusing cylindrical lens CL. In Figure 2-9, the long axis of the excimer laser beam is oriented vertically. Dark arrows indicate computer-controlled adjustments in angle and translations used to write gratings with different Bragg wavelengths. It was concluded that the new fabrication technique offered the possibility of cost-effect fabrication of high-strength, high-count arrays necessary for distributed sensing in smart structure applications.

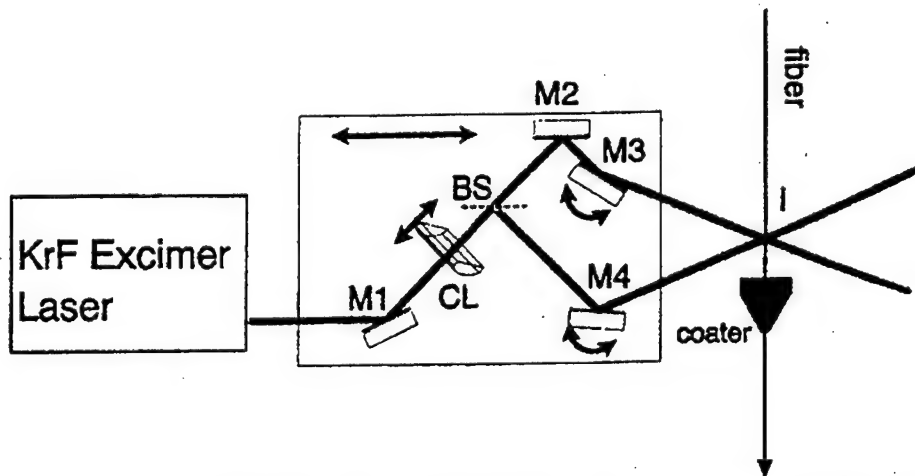


**Figure 2-9** Schematic diagram of the excimer laser interferometer used to write the gratings during the fiber draw  
(Askins et al, 1994)

A physical and mathematical model for tapped fiber optic Bragg grating sensors was developed by Perez et al. (1995b). The model for tapped Bragg gratings is useful in understanding the basic parameters needed to fabricate a tapped Bragg grating. To effectively fabricate tapped Bragg grating sensors, the Bragg angle and period need to be determined to scatter radiation out of the fiber at a desired scattering angle. In addition, other questions need to be answered. For example, how is the energy spread out of the fiber and what is the band pass of the scattered radiation? This information is also important to determine how many sensors can be placed in a single fiber.

Perez et al. divided their report into sections dealing with various aspects of the modeling effort. In section II, the model and the tapped Bragg grating fabrication parameters are described. In section III, the band pass of a Bragg grating sensor and the band pass of a tapped Bragg grating for two different fiber modes are calculated. In section IV, the Poynting Vector and Scattered Power are calculated, and section V shows how the energy is spread out of the fiber for two different fiber modes. An extensive mathematical analysis of the physical model was carried out and Perez et al. they concluded that the spectral width of a tapped Bragg grating is strongly dependent on the scattering angle. In addition, the spectral width of a tapped Bragg grating was found to be several orders of magnitude larger than the spectral width of a standard Bragg grating sensor. This significantly limits the number of tapped Bragg gratings that can be placed on a single fiber with independent interrogation. The spatial energy out of a fiber was derived, and

this result is expected to help guide future research on the development of, for example, a corrosion sensor.

The mechanical reliability of fiber optic Bragg grating sensors to be used for strain measurements was investigated by Sennhauser et al. (1996, 1997). A model was developed for sensor reliability and a series of aging tests was carried out at elevated temperatures, and at various relative humidity levels and stress levels. The optical fiber sensors in the tests were embedded in glass reinforced polymer composites or surface attached to carbon fiber reinforced polymer composites. It was concluded that with today's limited physical understanding of the aging process of fiber Bragg sensors, lifetime testing has to be performed with a well defined parameter set relevant to the actual sensor application and environmental conditions. Factors that accelerate aging such as elevated temperature, humidity, action concentration and mechanical stress levels need to be considered.

The development of a new multi-axis strain sensor that has the capability to measure both axial and transverse strains when embedded in a structure has been reported by Udd et al. (1998, 2000). The multi-axis sensor is formed from dual gratings written on polarization preserving fiber. [A more detailed description of these sensors and their application to adhesive joint monitoring will be given in Section 3.6 of this Technology Assessment].

The reliability has been investigated of commercially available optical fiber Bragg grating sensors when used at elevated temperatures as strain and temperature sensors (Sennhauser et al. 2000). The mechanical and optical reliability of commercial fibers and commercial Bragg gratings was modeled at elevated temperatures up to 230 degrees C. Sennhauser et al. experimentally tested the mechanical reliability and optical reliability of the Bragg gratings; Table 2-1 shows the conditions used to study the commercially available polyimide re-coated fiber optic Bragg gratings. The automated tensile test apparatus illustrated in Figure 2-10 was used to carryout the experiments on the fiber optic Bragg gratings in an argon atmosphere. The mechanical and optical reliability was determined for two commercial types of Bragg gratings and it was concluded that the methodology could be used to monitor commercial Bragg grating production.

Table 2-1 Environmental operation conditions for polyimide re-coated fiber optic Bragg grating  
(Sennhauser et al, 2000)

temperature range	100 °-230 °C
temperature resolution	≤ 1 °C
strain range	0 – 10'000 µm/m
strain resolution	≤ 1 µm/m
operation time	≥ 5 a
atmosphere / dew point	inert gas / ≤ -30 °C
fiber and BG coating	polyimide

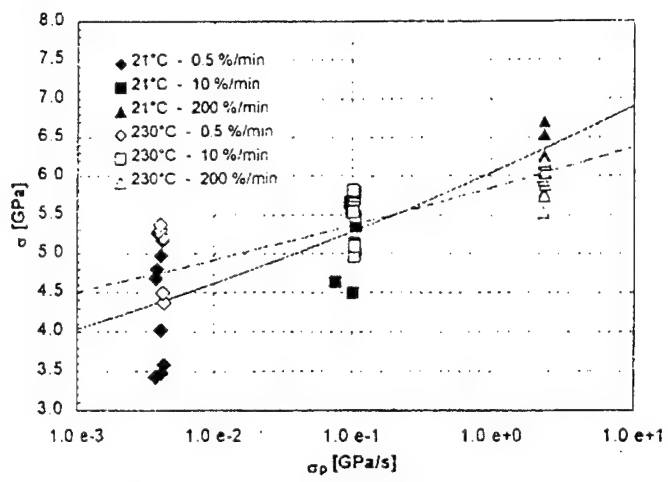


**Figure 2-10** Fracture stress versus stress rate and 50%-quantile fits for pristine fiber A at 21°C (filled symbols) and 230°C (open symbols)  
(Sennhauser et al, 2000)

### 3.0 REVIEW OF REPORTED APPLICATIONS

This section contains a review of the reported applications of Bragg grating sensors. The principal applications have been: determination of temperature and strain, monitoring of composites, large civil structure monitoring, sensing for acoustic emission, monitoring of adhesive joints, chemical sensing, and corrosion detection.

#### 3.1 Determination of Temperature and Strain

As mentioned in Section 2.0, in one of the earliest works on Bragg grating sensors, Meltz, et al. (1987) developed a twin-core, polarimetric, in-fiber Bragg grating temperature and strain sensor. A twin-core sensor was used in the form of a differential interferometer that was shown earlier in Figure 2-1. Both temperature and strain could be measured at the same time as shown in Figure 3-1 by utilizing two different wavelengths. It was concluded that the in-fiber Bragg grating sensors provide a new means for making quasi-distributed measurements of temperature and strain in composite materials as shown schematically in Figure 3-2.

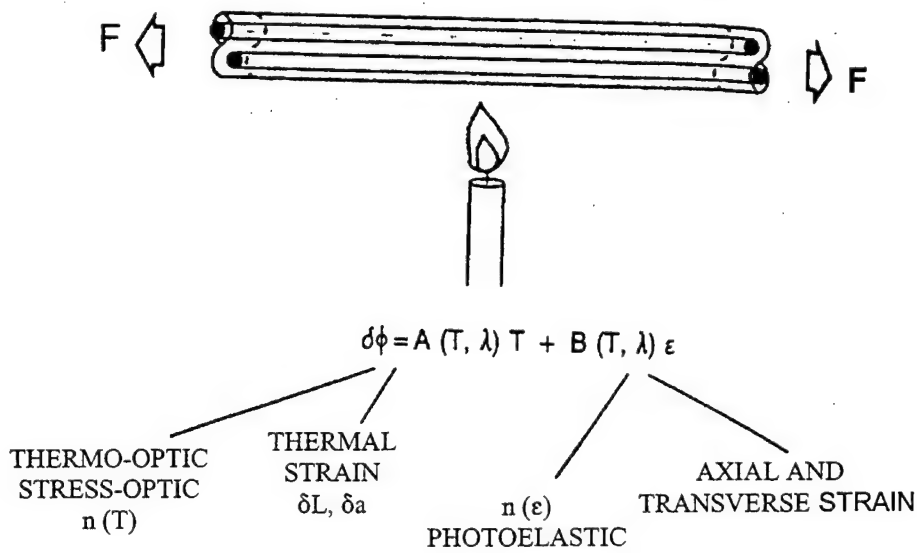


**Figure 3-1** Contributing factors to temperature and strain sensitivity. Note the wave length dependence of the coefficients  
(Meltz et al, 1987)

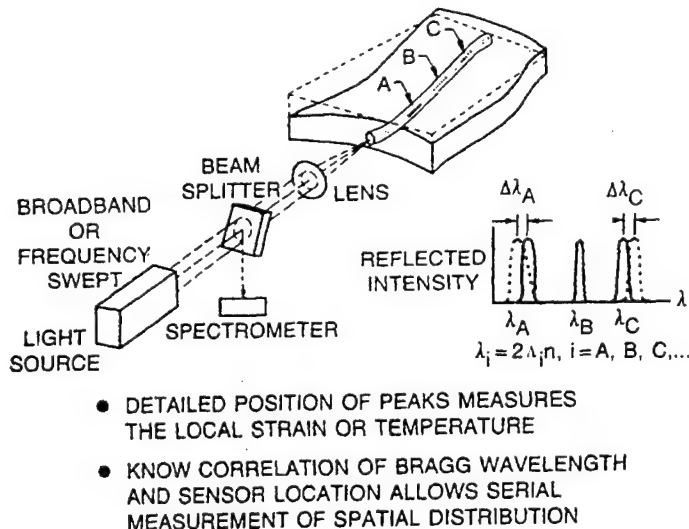


**Figure 3-2** Technique for quasi-distributed strain sensing using in-fiber Bragg gratings  
(Meltz et al, 1987)

A fiber optic Bragg grating differential temperature sensor was reported by Kersey and Berkoff (1992). This system is based on an unbalanced interferometer as a wavelength discriminator to provide high sensitivity to thermally induced Bragg wavelength shifts of the sensing gratings as shown in Figure 3-3. A broad band light source (Er-doped superfluorescent fiber source) was used coupled through an unbalanced Mach-Zehnder Interferometer with a fiber path imbalance of about 3.0 mm. The arms of the interferometer were wound on piezoelectric transducers that allowed biasing and/or modulation of the interferometer phase. The gratings were placed in individual thermal enclosures to allow for differential temperature adjustment. Figure 3-4a shows the phase difference that the authors measured for various differential temperatures and Figure 3-4b shows the resulting linear plot of the data. It was concluded that differential temperatures could be measured with a resolution better than 0.05 degrees C with a range of about 60 degrees C.

A technique to measure strain for smart structures was developed by Measures et al. (1992). In this effort, the wavelength encoded narrowband output of a fiber Bragg grating strain sensor was split into two paths. In one path the intensity was directly measured while in the other, the light passed through a bulk optic wavelength dependent filter before reaching a detector. Provided the filter cut off is close to the Bragg wavelength, the ratio of the two intensities then provides a determination of the wavelength and hence the strain.

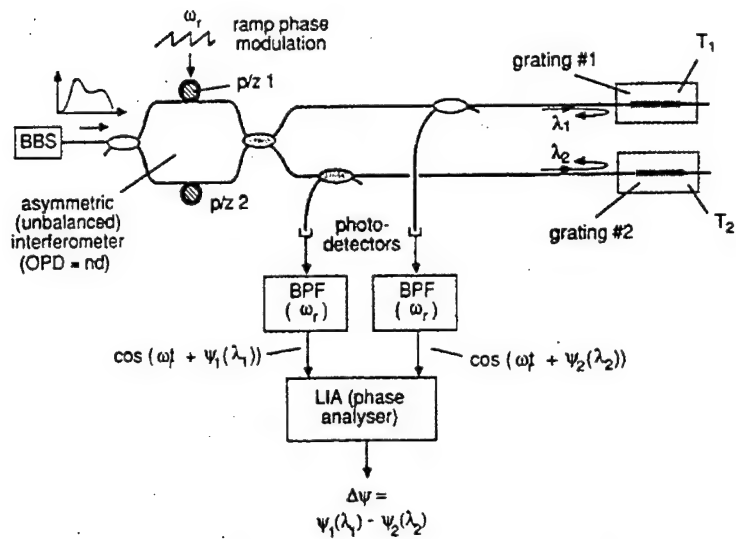
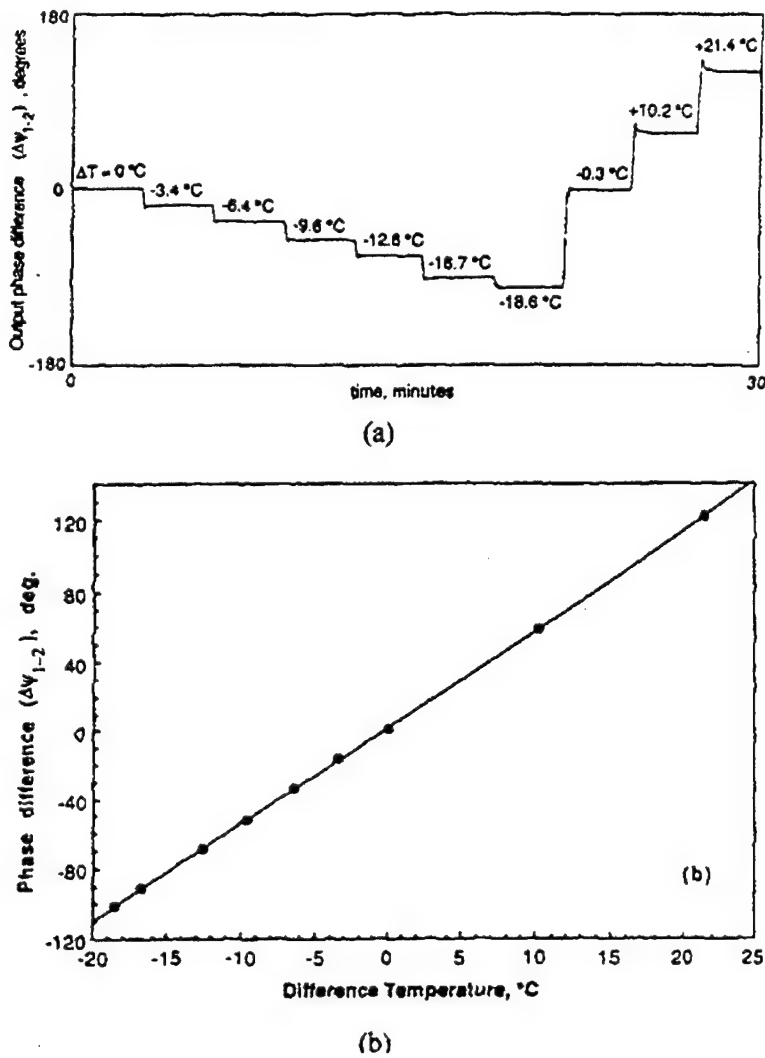
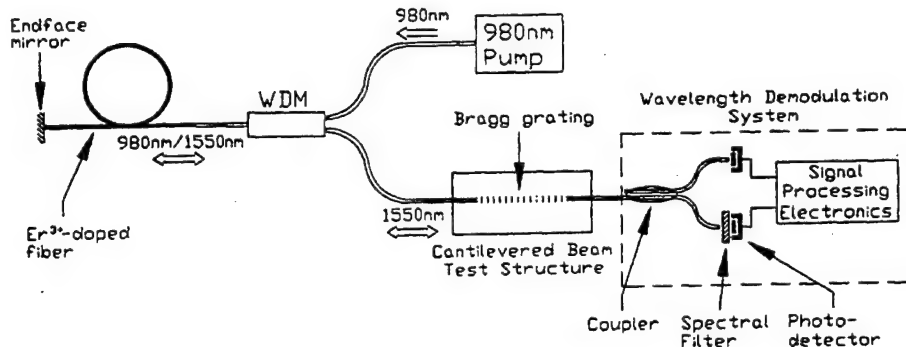


Figure 3-3 Fiber optic Bragg grating based differential sensor system  
(Kersey and Berkoff, 1992)

Development of a fiber laser sensor system that permits efficient interrogation of Bragg grating sensors was reported by Melle et al. (1993). A schematic illustration of this system used as a strain sensor is shown in Figure 3-5. Pumped light from a diode laser operating at 980 nm is coupled to a length of erbium-doped fiber. A broadband mirror reflects the unabsorbed portion of the pumped light after a first pass through the doped fiber, increasing the absorption efficiency of the system. A fiber with an intracore Bragg grating is fusion spliced to the arm of the wavelength division multiplexer that passes only 1550 nm light. The grating provides the necessary reflection for lasing to occur. The broadband mirror and the Bragg grating reflector define the laser cavity. The use of a broadband mirror as one cavity reflector permits the fiber laser to be tuned without requiring both reflectors to be in the same strain or temperature state. This is an advance over systems that use two Bragg gratings as cavity mirrors and require them to be at the same temperature or strain state. The Bragg grating can therefore be located remotely from the doped fiber, allowing it to be adhered to, or embedded within, a structure under test. Finally the output light from the fiber laser is coupled to a passive wavelength demodulation system which is used to determine the laser wavelength.



**Figure 3-4** (a) Phase difference output recorded over a 30 min period for various differential temperatures applied to the gratings (b) Plot of the data of (a) (Kersey and Berkoff, 1992)



**Figure 3-5** Schematic of the fiber laser strain sensor system (Melle et al, 1993)

Results that relate fiber laser output wavelength as a function of strain on the Bragg grating are shown in figure 3-6. Melle and coworkers used the system to track the results of a step input excitation of an aluminum beam. It was concluded that the system provides interrupt immune strain sensing with a high resolution and a bandwidth of 13.0 kHz. Melle et al. expected that future developments would lead to a system with an array of embedded sensors for smart structure applications.

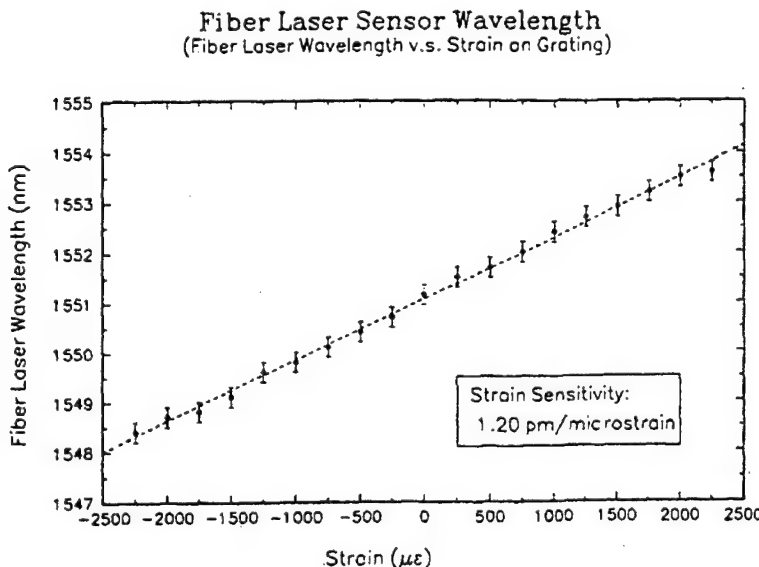


**Figure 3-6** Fiber laser output wavelength as a function of strain on the Bragg grating  
(Melle et al, 1993)

A fiber Bragg grating strain sensor using a wavelength division coupler with a monotonic transfer function was reported by Davis and Kersey (1994). The work was an effort to improve on the earlier work that used a bulk demodulation approach (Measures et al. 1992). Davis and Kersey believed that the earlier work: (1) required extreme care to prevent unwanted reflections and power loss in the sensing system; and (2) the use of a filter inherently causes signal intensity loss that may not be acceptable in large multiplexed systems with low power levels. To overcome these problems, a simple, all fiber implementation of the wavelength discrimination principle using a wavelength dependent  $2 \times 2$  fiber optic coupler was used. Figure 3-7 shows the strain sensing configuration used by Davis and Kersey. Detection of the output intensity of both ports on the output coupler and simple electronic processing reveals a voltage directly proportional to the grating strain. Electronic processing of the two detected power levels consisted of taking the ratio between the difference of the outputs and the sum of the outputs to normalize for intensity variations. It was concluded that by effectively eliminating intensity variation effects the advantageous intensity insensitivity operation of the fiber Bragg gratings is maintained.

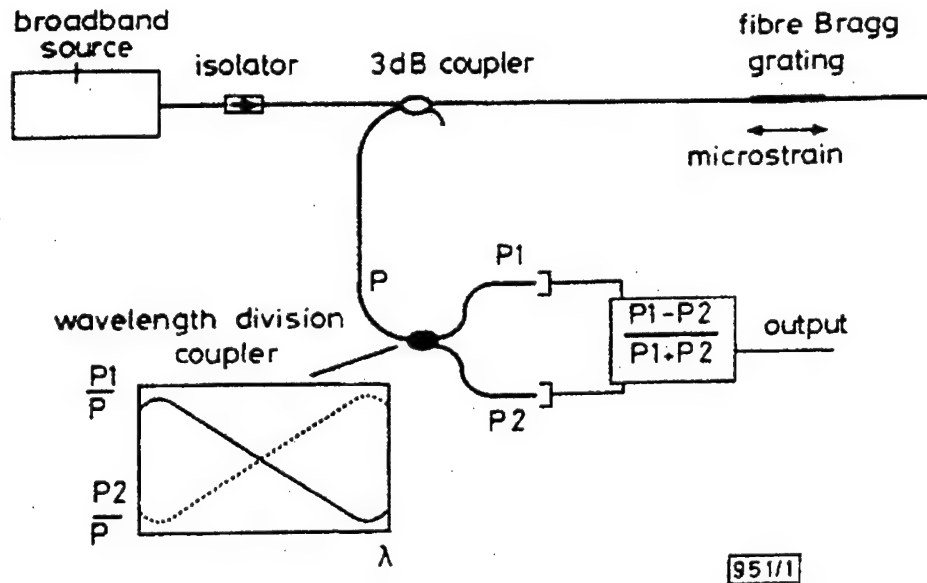


**Figure 3-7** Diagram of strain sensor configuration using a fibre Bragg grating and wavelength division coupler  
 (Davis and Kersey, 1994)

Figure 3-8 shows results for induced strains up to 1050 microstrain. A conventional resistive strain gauge mount is used alongside the grating to provide calibration. The data indicate a static strain resolution of about plus or minus 3 microstrain, and a dynamic strain resolution of about 1 microstrain for the sensing system. Davis and Kersey concluded that this was about two orders of magnitude better than previous grating demodulation systems had obtained. They were able to obtain a linear response of the sensor to applied strains over a 1000 microstrain sensing range. They also concluded that their multi fiber sensing system might be easily multiplexed so that only one coupler is needed to service all gratings in an array. This would be done via time division multiplexing and wavelength division techniques.

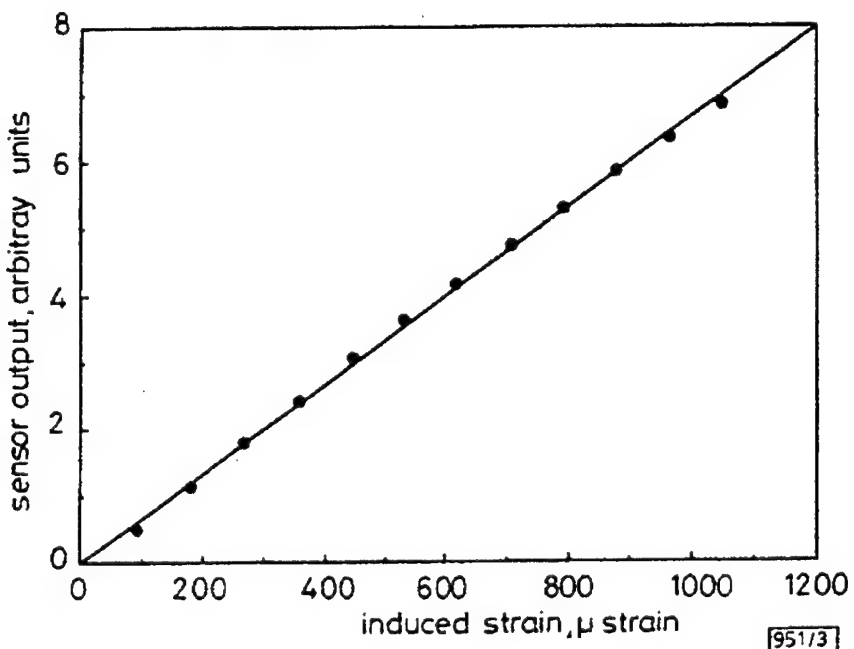


**Figure 3-8** Response of sensor output voltage to three-point bending induced strain  
(Davis and Kersey, 1994)

The properties and performance of a number of optical fiber-based long-period and Bragg grating temperature, strain, and refractive index sensors were investigated by Bhatia et al. (1996). The work was motivated by the U. S. Navy's desire to use robust, inexpensive fiber sensors which could be embedded in machinery (metal structures) to make strain and temperature measurements for machinery health monitoring. Bhatia et al. compared the magnitude of the spectral shift of the resonance bands, cross-sensitivity to undesired perturbations, bend sensitivity, and the ease and cost of demodulating the grating signal. Long-period gratings were fabricated as well as Bragg gratings in five different types of optical fibers: AT&T standard dispersion-shifted fiber, conventional 1310 nm fiber, 980 nm single mode fiber, Corning FLEXCOR fiber, and standard 1320 nm fiber. Bhatia et al. viewed Bragg gratings as elegant in-fiber sensors particularly suitable for multiplexed and distributed applications. However, Bragg grating sensors have limited spectral shift due to strain and temperature effects and often require complex interferometric techniques to detect wavelength shifts. In addition, Bragg grating sensors often require etching of the cladding to gain access to the evanescent field of the guided wave. Bhatia et al. described long-period grating sensors that were developed for communications systems as an alternative to Bragg grating sensors for temperature, strain, and refractive index measurements.

Bhatia and coworkers compared the sensors in a series of tests to determine their attributes and disadvantages. They concluded that the long-period gratings possess spectral shifts that are strong functions of the fiber parameters. All five different long-period grating sensors had temperature coefficients larger than that for Bragg grating sensors. In addition, long-period grating sensors do not require etching of the cladding unlike Bragg gratings. This maintains the strength and durability of the sensors and

makes them less susceptible to damage under harsh environmental conditions. Long-period grating sensors are sensitive to small bends and this could be a disadvantage compared to Bragg grating sensors. Long-period grating strain and refractive index sensors are limited by their cross sensitivity to ambient temperature changes. However, long-period grating sensors offer simple demodulation techniques that can be relatively inexpensive to implement.

### 3.2 Composite Processing

Lawrence, et al. (1996) investigated the measurement of process-induced strains in composite materials using two types of embedded sensors: fiber optic Bragg grating sensors and extrinsic Fabry-Perot interferometers. The optical sensors and thermocouples were embedded in graphite/epoxy composite laminates prior to cure. The specimens were then cured in a press while the internal strains and temperatures developed during processing were monitored. Figure 3-9 shows the extrinsic Fabray-Perot interferometer used for strain measurements and Figure 3-10 shows the Bragg grating sensor. The Fabray-Perot has the advantage that it is relatively insensitive to strains transverse to the longitudinal axis of the fiber and to temperature changes. These sensors can be used for point measurements, but are difficult to manufacture and calibrate. They are also larger in diameter than typical lead-in fibers which can create difficulties for embedded applications. One disadvantage of the Bragg grating sensor is that it is not possible to separate the effects of applied strain and temperature changes with a single grating. Bragg grating sensors are also sensitive to strains transverse to the fiber axis and to shear strains because of the strain optic or photoelastic effect.

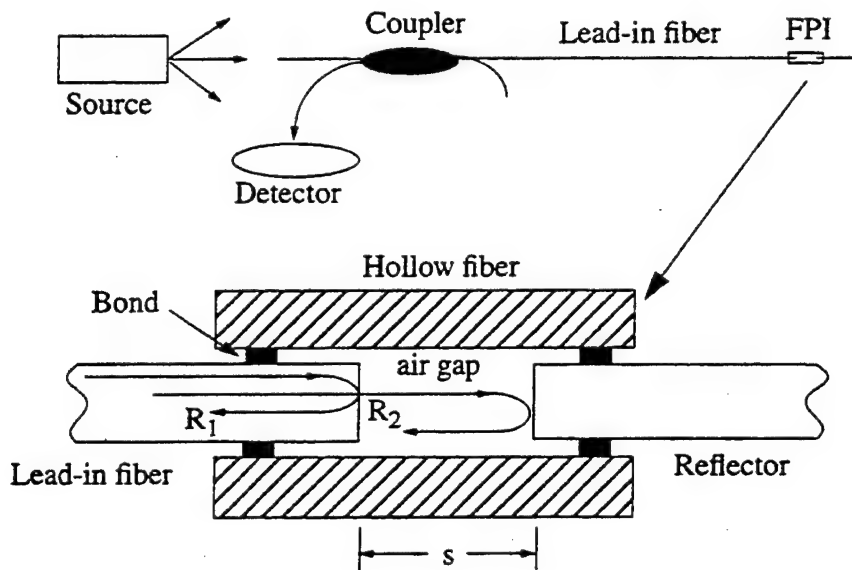


**Figure 3-9** Extrinsic Fabry-Perot interferometer for the measurement of strain  
(Lawrence et al, 1996)

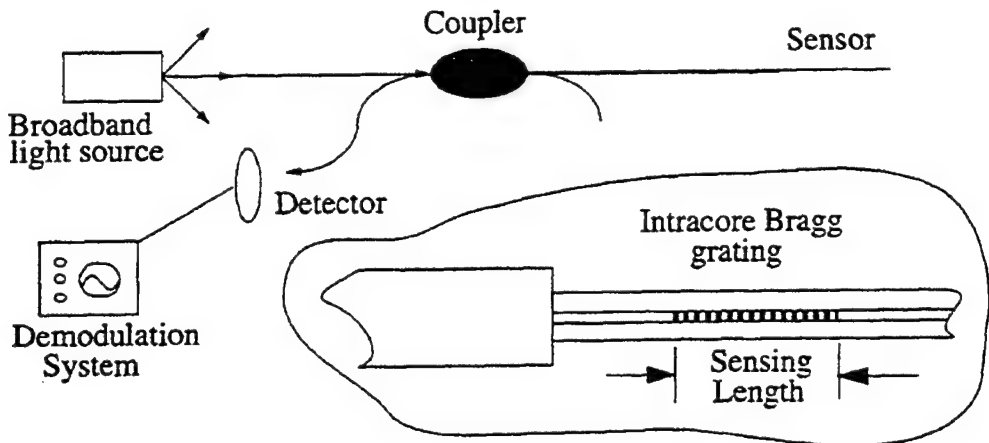


**Figure 3-10** Bragg grating fiber optic sensor for measurement of strain  
 (Lawrence et al, 1996)

Lawrence and coworkers determined the process induced strains shown in Figure 3-11 with the Bragg grating sensor corrected for thermal changes. The correction factor used was 5.3 microstrain/ $^{\circ}$ F. They also determined the process induced strains shown in Figure 3-12 with the extrinsic Fabry-Perot interferometer. It was concluded that the chemical and thermal shrinkage strains internal to a composite part during cure processing could be nondestructively measured with this method.

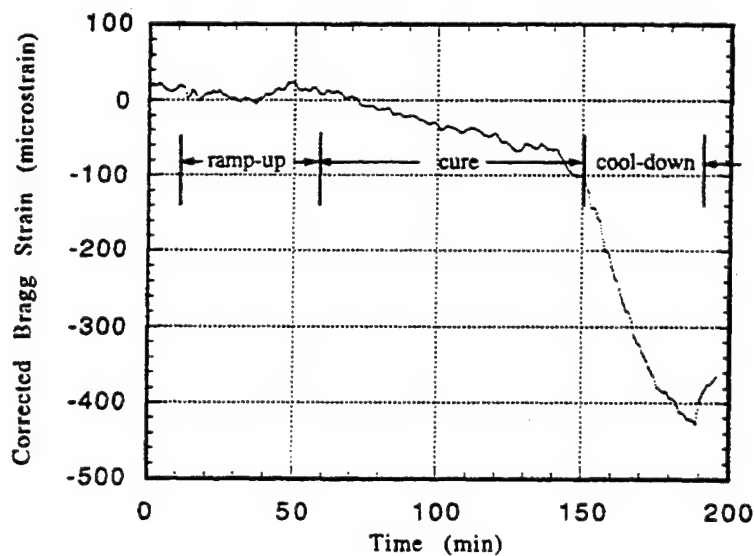


**Figure 3-11** Output of Bragg grating sensor during cure corrected for thermal apparent strain  
 (Lawrence et al, 1996)

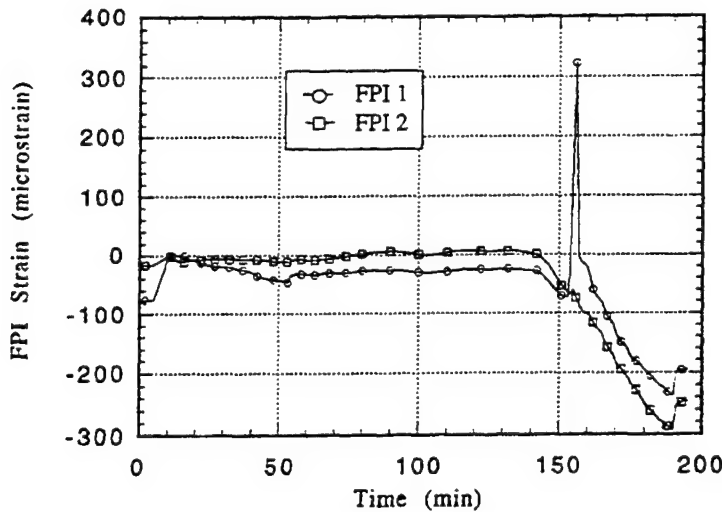


**Figure 3-12** Process induced strains measured with the extrinsic Fabry-Perot interferometers  
 (Lawrence et al, 1996)

Investigations have been performed on using Bragg grating sensors to monitor the curing of composites (Slattery et al. 1998). The cure cycle of composites is quite complex and the studies with Bragg grating sensors during resin infusion and cure were aimed at improving the understanding of the process. Residual stresses resulting from the thermal expansion coefficient of the fiber being generally much lower than that of the polymer matrix are induced in fiber composites during the cure process. The two materials are locked together at the cure temperature and as they cool, the matrix attempts to contract more than the fiber leading to tension in the matrix and compression in the fiber. This can lead to the formation of microcracks parallel to the fibers in thick composite plies or yarns. Optimizing the cure cycle can reduce the magnitude of the residual stress.

Slattery et al. used test panels of fiberglass/epoxy that were 12 in x 24 in x 1 in thick, with 108 plies. Two fiber optic Bragg grating sensors were embedded, one at the center of the panel and the other four plies from the tool interface. The output of the sensors was measured using a spectrum analyzer to determine changes in wavelength. The spectrum analyzer provides high strain resolution of about 10 microstrain and must be capable of resolving 0.01 nm in wavelength. A commercial demodulator (Blue Road Research) that is based on the comparison of two light output intensities was used. The commercial demodulator is less expensive than a spectrum analyzer, has about an order of magnitude less wavelength change sensitivity, but has a much higher sampling rate capability (hundreds of kHz compared to a few Hertz). Preliminary, micromechanical finite element analysis was also performed to study the development of residual strain gradients along the Bragg grating.

Slattery et al. concluded that their work demonstrated the potential in using embedded optical fiber sensors for cure monitoring and later health monitoring of composite structures. They found that the sensors were able to precisely indicate the temperature

increase in the part during heating, the onset of the gel stage of the cure, and the completion of curing at multiple points and planes in the composite panel. Residual strain and strain gradients could be measured after cool down.

The use of embedded fiber optic sensors in smart pultruded fiber reinforced composites was investigated by Kalamkarov et al. (1998). Fiber Bragg grating sensors and fiber Fabry Perot sensors were successfully embedded in composites during the pultrusion process. Since the Bragg grating sensors showed a greater survivability in the pultrusion process than the Fabry Perot sensors, only the Fabry Perot sensors needed to be reinforced to enhance survivability. Carbon and glass fiber reinforced polymer composite rods 9.5 mm in diameter were pultruded using a urethane modified vinyl ester resin system known for its good mechanical properties and excellent process-ability. During dry pultrusion, the output of the sensors was obtained and found to conform quite well to the temperature profile within the die. Figure 3-13 shows the output of a Bragg grating sensor during normal and dry pultrusion.

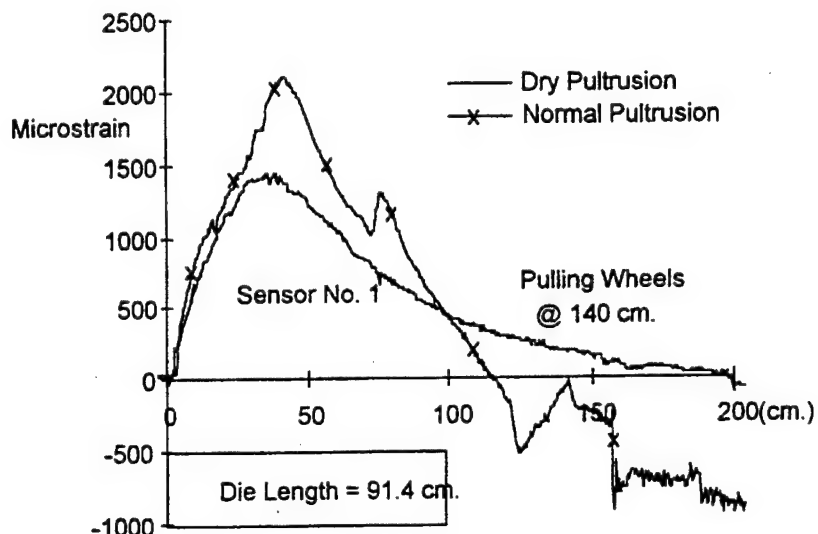


**Figure 3-13** Comparison of output from Bragg grating sensor during normal and dry pultrusion  
(Kalamkarov et al, 1998)

Kalamkarov et al. also tested the smart tendons produced in the pultrusion process in a testing regime using a load cell. Figure 3-14 shows the experimental setup used. A commercial (RocTest Ltd.) demodulation unit was used to record the strain from the Fabry Perot sensors, and a commercial (BIS 1000) PC card was used to record the strain from the Bragg grating sensors. Figure 3-15 shows strain versus time from an extensometer and an embedded Bragg grating sensor in a glass composite tendon subjected to a sinusoidal load. An embedded fiber Fabry Perot sensor, which had been reinforced to strengthen it, was also tested and the results were somewhat better than those obtained from the Bragg grating sensor. Kalamkarov et al. concluded that Fabry Perot and Bragg grating fiber optic sensors are useful in characterizing the pultrusion process. In addition, embedded optical fibers have no significant effect on the tensile

properties of pultruded composites, but they do slightly deteriorate the shear strength of the composites. The mechanical testing of the smart tendons was successful in demonstrating the capability of the fiber sensors to monitor the strain in the tendons although some discrepancies were observed.

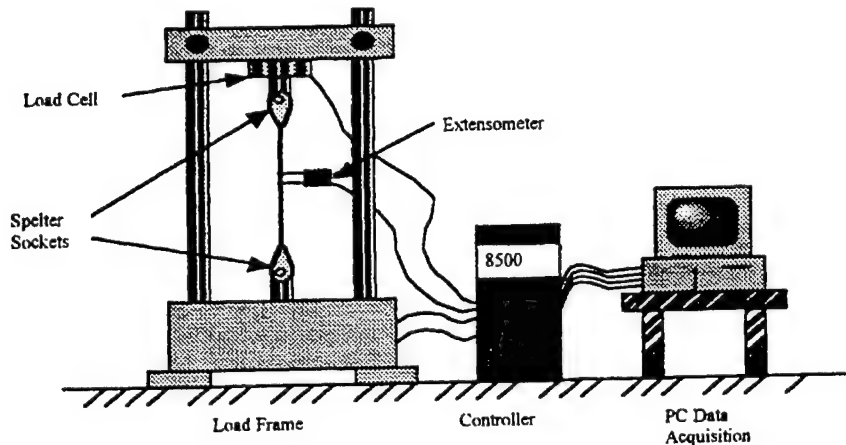


**Figure 3-14** Experimental setup for mechanical testing of pultruded tendons  
(Kalamkarov et al, 1998)

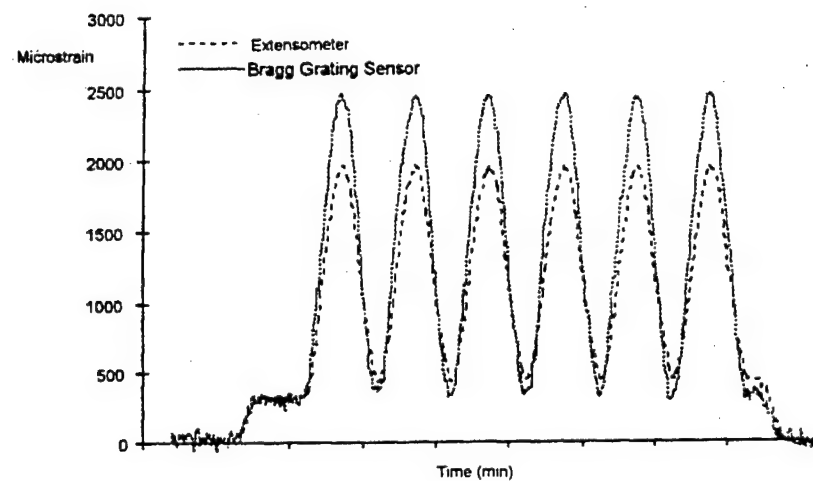


**Figure 3-15** Strain vs. time plot from extensometer and embedded Bragg grating sensor in a glass composite tendon subjected to a sinusoidal load  
(Kalamkarov et al, 1998)

### 3.3 Monitoring of Civil Structures

The use of fiber optic Bragg grating sensors to monitor the variation in strain due to flexural deformation in prestressed concrete structures was investigated by Maher et al. (1993). Both embedded and surface mounted sensors were used to monitor the strain in prestressed concrete beams. Conventional electrical strain gauges were also attached to

the tendons for comparison. Three point bending tests were performed on 3.05 m-span, prismatic, high strength reinforced concrete beams having a T-shape cross section. Finite element modeling was used to evaluate the strain transfer process in the attachment of the sensors and it was determined that using a very thin film of high elastic modulus epoxy for the attachment gave the best strain transfer. Figure 3-16 shows the strain data for the Bragg grating sensor as compared to the strain gauge, and a very good relationship is observed. Maher et al. concluded that the results of their laboratory study showed that Bragg grating fiber optic sensors could be used for quantitative measurement of strain in pre-stressed concrete structural elements undergoing flexural deformation.

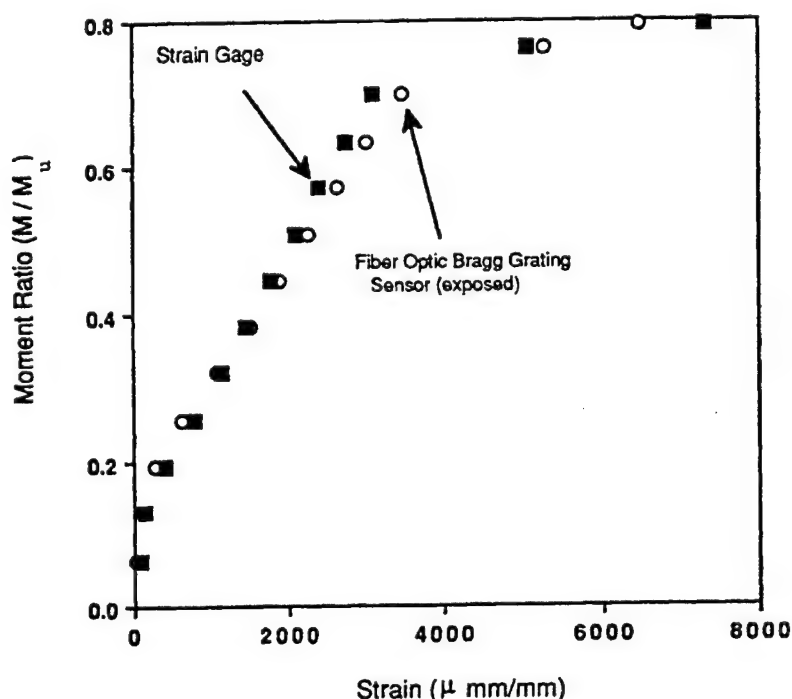


**Figure 3-16** Moment ratio vs. tensile strain on fiber optic Bragg grating sensor embedded in a large scale T-shaped concrete beam  
(Maher et al, 1993)

A detailed investigation on the use of fiber optic Bragg grating sensors for the nondestructive evaluation of composite concrete beams was carried out by Chen et al. (1994). Both attached and embedded sensors were used to monitor and obtain strain data from an array of twelve high strength composite concrete beams. It was found that fiber optic Bragg grating sensors could be successfully used for accurate, quantitative, and at the same time nondestructive monitoring of the behavior of composite concrete beams under long-term service loads, with the ability to warn against impending failure. Chen et al. found that the sensors show high sensitivity and accuracy in average strain measurements in reinforcement, and in evaluating the flexural stiffness of the structural components in constructed concrete facilities. Crack widths at service loads can also be evaluated. Figure 3-17 shows crack width measurements obtained from Bragg grating sensors as compared to micrometer measurements of the crack. The 45-degree slope

indicates that the total elongation of the reinforcement is approximately equal to the total stretch of the concrete.

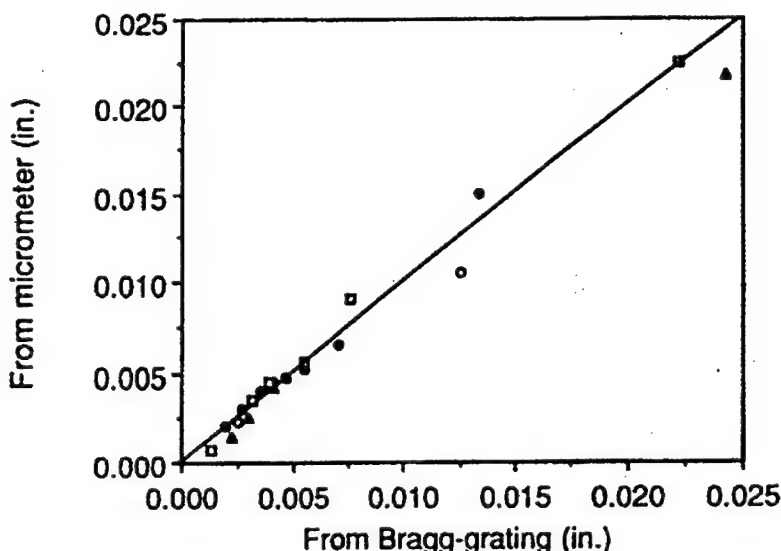


**Figure 3-17** Average crack-width measurement obtained from fiber optic Bragg grating sensors and micrometer  
(Chen et al, 1994)

Fiber optic sensors have also been investigated for the nondestructive strength evaluation and early warning of impending failure in structural concrete components transforming them into smart systems (Nawy 1995). The optical system shown schematically in Figure 3-18 was used to measure the strain in the components. An edge light emitting diode at 1300 nm was used as a broad band light source to provide the required wavelength region. A commercial optical spectrum analyzer, ANDO AQ6310B was used to measure the reflected Bragg wavelength. Figure 3-19 shows the typical shift in wavelength as a result of strain on the component and on the sensor. A total of twenty-one large-scale structural elements covering reinforced/prestressed and composite concrete types were tested. Bragg grating sensors were both embedded in the concrete and mounted on the surface, and electric foil strain gauges were also used for comparison. Load induced strains were measured with the Bragg grating sensors and the electric foil sensors. Navy concluded that Bragg grating sensors could be successfully used to quantitatively monitor strain/stress in either new or existing concrete components. This provides for the accurate nondestructive monitoring of the composite concrete member under long-term service loads, with the ability to warn against impending service failure. Unlike mechanical extensiometers, fiber optic Bragg grating sensors are flexible and can be set to any desired gauge length which can arrest at least two cracks in large scale concrete members.

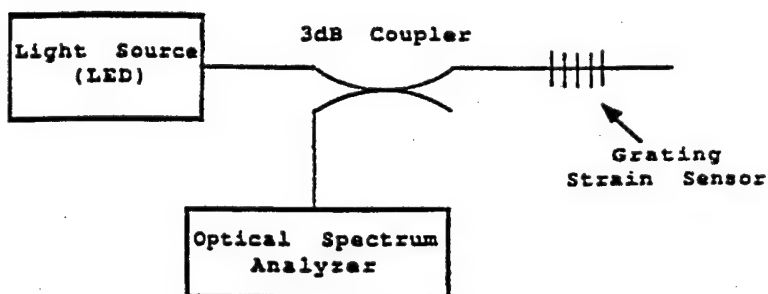


**Figure 3-18** Optical measurement system fiber optic Bragg grating sensor for strain measurement  
(Nawy, 1995)

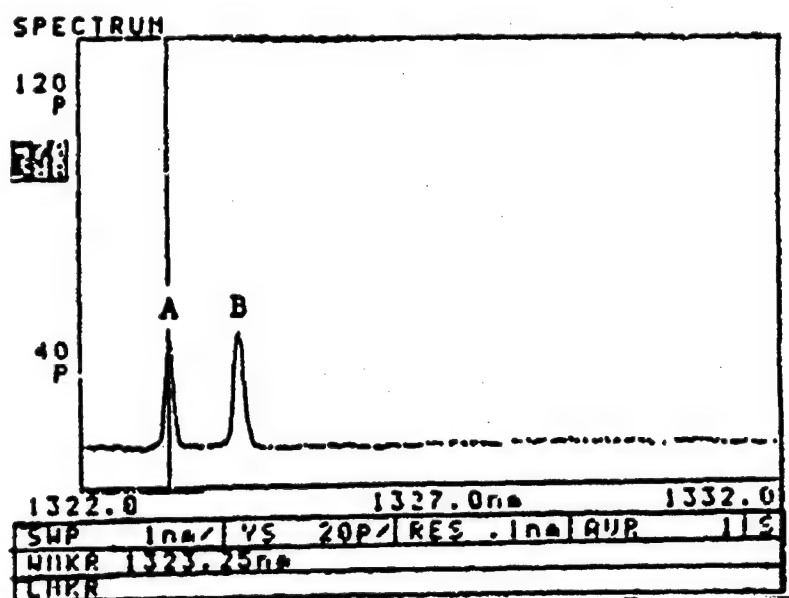


**Figure 3-19** Typical wavelength shift (from point A to point B) as a result of strain on fiber optic Bragg grating sensor  
(Nawy, 1995)

Two additional Bragg grating fiber optic sensor systems for bridge monitoring were developed by Davis et al. (1996a, 1996b). The first sensor system is capable of assessing long-term static structural loading changes and the second sensor system monitors dynamic/modal behavior of the structure. This is accomplished by using two different optical interrogation schemes to address the same sensor array. Forty-eight fiber Bragg grating sensors were deployed in a quarter-scale single lane bridge span and the sensors interrogated with the two separate systems, which permitted static or dynamic strain information to be obtained from each sensor.

Davis et al. (1996a, 1996b) used the system shown schematically in Figure 3-20 to monitor the static strain in the bridge. A single 1.3 micrometer edge light emitting diode source with about 150 microwatts of power was used to illuminate 5 arrays of 12 fiber Bragg sensors. The strings of sensors were illuminated sequentially through a 3 dB coupler and two single-mode optical fiber switches. The system is under PC control and is capable of addressing 64 strings of sensors. The light reflected from the grating sensors is returned to a scanning Fabry-Perot (FP) optical filter and then to a detector. The system shown schematically in Figure 3-21 was used to monitor the dynamic response of the bridge. A broadband edge light emitting diode provides the broadband spectra, which is filtered by an adjustable bandpass optical filter. This permits only one Bragg grating sensor to be illuminated at a time. The reflected light from the Bragg grating sensor is then directed into the wavelength division multiplexer. The tunable optical filter permits any number of fiber Bragg grating sensors on a single optical fiber to be sequentially interrogated. The use of a multi-port filter would allow several sensors to be addressed simultaneously, for multiplexing operations of this dynamic sensing approach. This is a complex optical device and Davis et al. provided a detailed description of the optical mechanisms involved.

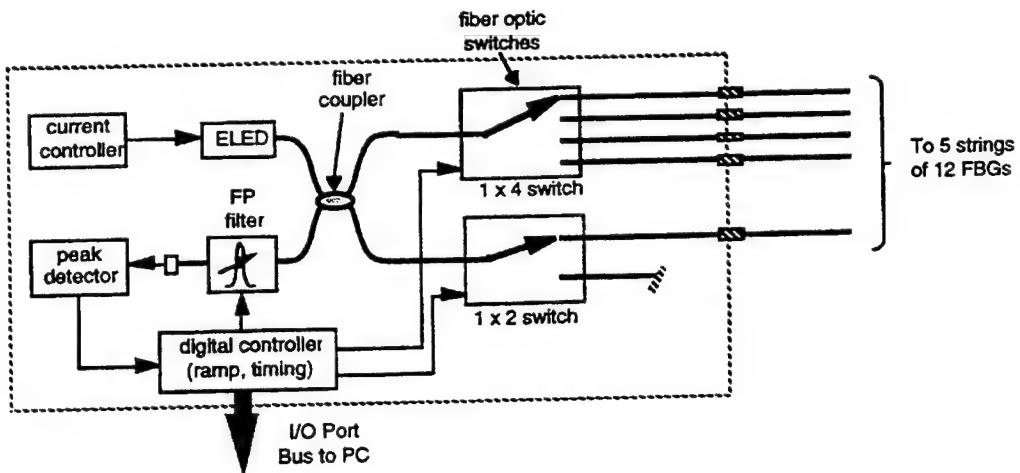


**Figure 3-20** Schematic diagram of the 60 channel fiber Bragg grating (FBG) sensor electro-optics system for monitoring strain in bridges  
(Davis et al, 1996)

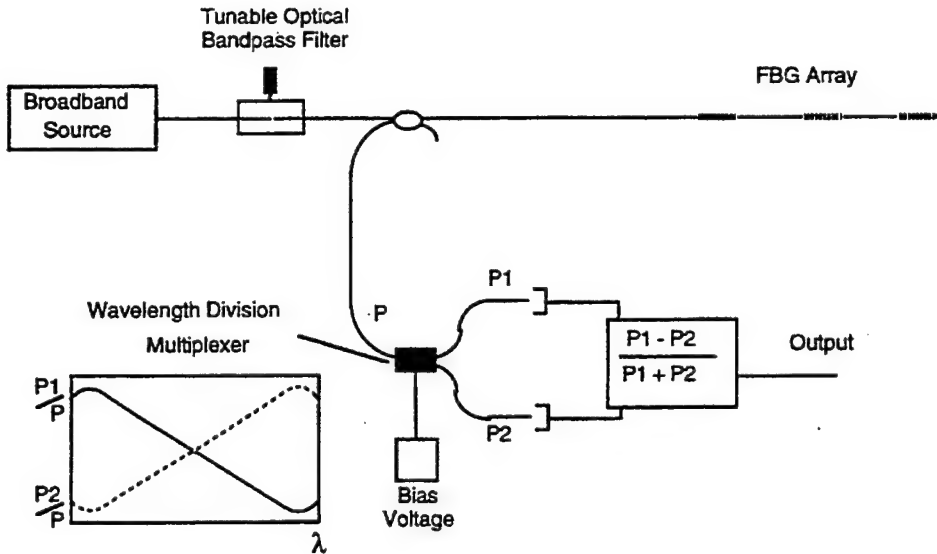


**Figure 3-21** Schematic diagram for the dynamic fiber Bragg grating (FBG) bridge interrogation system  
(Davis et al, 1996)

Davis et al, embedded thirty Bragg grating sensors in the bridge deck and attached 17 Bragg grating sensors to the steel I-beams as shown in Figure 3-22. Figure 3-23 shows the placement of the sensors in the concrete deck attached to the rebar before the concrete was poured, and Figure 3-24 shows the placement of the sensors attached to the I-beams. Davis et al. concluded that the systems were stable over a period of 38 days and monitored the 48 strain sensors embedded and attached to the bridge. The pouring and setting of the concrete, and static loading of the bridge were monitored. In addition, the dynamic response of the bridge was monitored after it was damaged and after it was repaired with a noticeable difference in the modal behavior of the bridge.

Jones, et al. (1996) reported on cantilever honeycomb plate monitoring using wavelength division multiplex fiber Bragg grating sensors. The cantilever honeycomb plate was similar to the type used on Navy satellites. An algorithm was developed to determine deformations of a cantilever honeycomb plate under arbitrary loading conditions. The algorithm utilizes strain information obtained from a set of sixteen fiber Bragg grating sensors mounted on the plate so that all sensor measure strain along the clamped-free direction. A wavelength division multiplexing system was used with the sensors. Jones et al. concluded that their method of determining accurate full field deformation information for plate structures using limited strain information and a least squares fitting algorithm was successful. Strain and displacement data from a finite element model were used to determine the optimum measurement locations for the sensors.

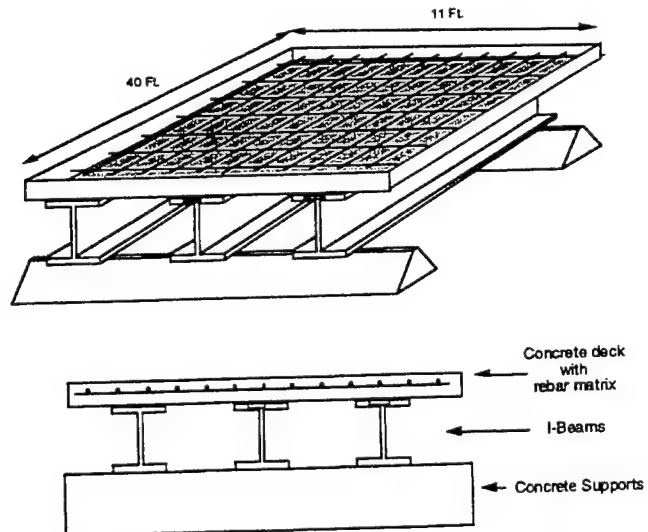


**Figure 3-22** Schematic of bridge section

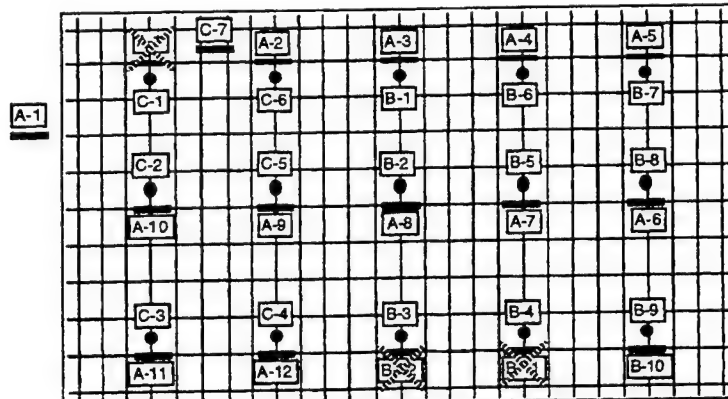


**Figure 3-23** Fiber Bragg grating sensor placement in concrete deck  
(Davis et al, 1996)

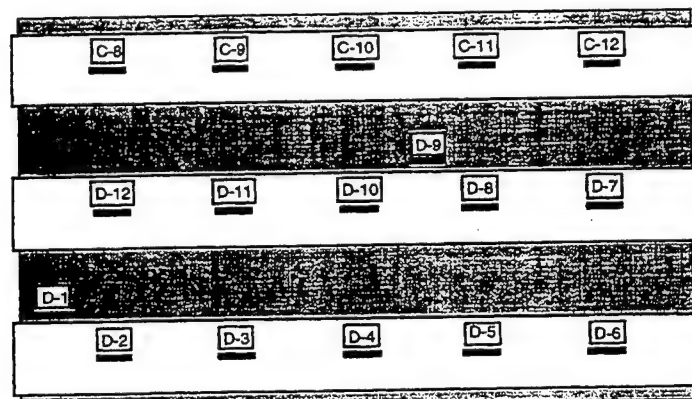


**Figure 3-24** Fiber Bragg grating sensor placement under steel I-beams  
(Davis et al, 1996)

The damage assessment of a full-scale laboratory bridge using a network of distributed optical fiber Bragg grating sensors was reported by Kodindouma et al. (1996). This study was associated with the work reported earlier by Davis, et al. (1996a). Kodindouma et al. monitored the bridge before and after a series of cuts were introduced in an external girder to simulate a fatigue crack. The after fracture behavior of the bridge is described in terms of load path redistribution and strain level changes in the structure.

Nawy and Chen (1996) investigated the application of Bragg grating fiber optic sensors for monitoring the behavior of continuous composite concrete beams reinforced with prestressed prisms. This investigation was an extension of the research by Navy (1995) discussed earlier. Navy and Chen discuss the investigation of continuous beams that were loaded to failure. The experimental results obtained with Bragg grating sensors are compared with theoretical evaluations obtained from nonlinear analysis. Navy and Chen concluded that their study provided new insight into the mechanical behavior, including cracking and failure, of continuous composite concrete beams.

The capability of Bragg grating sensors to monitor structural damage in composite-confined concrete columns was reported by McCollum and Slattery (1998). This effort focused on concrete columns that have been either retrofitted with fiberglass or carbon fiber composite over wraps to enhance mechanical properties. Bragg grating sensors were chosen as potential monitors because they appeared to be the most promising due to survivability, indication of absolute strain, cost and multiplexing capability. The study used both small-scale 2 inch diameter by 4 inch long confined concrete cylinders and large 12 inch diameter by 8 foot long cylinders. As shown in Figure 3-25, sensors were placed as hoop and axial gauges.

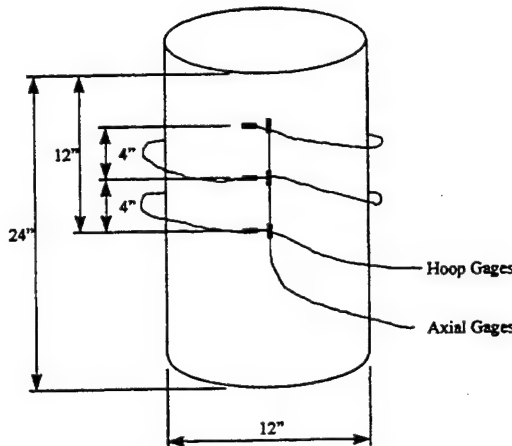


**Figure 3-25** Sensor placement in concrete cylinders  
(McCollum and Slattery, 1998)

An indicated strain versus strain state model was developed and micromechanical finite element simulations carried out to understand the strain states in the columns. The axial and hoop strain results from resistive and Bragg grating sensors were experimentally determined. Figure 3-26 shows a comparison of axial strain gauge results, and Figure 3-27 shows the comparison of the hoop strain gauge results. McCullum and Slattery

concluded that the Bragg grating gauges and resistive strain gauges showed significant differences in the indicated strain. The modeling effort could only account for part of this variation. However, it was concluded that the strain measurements with the Bragg grating sensors were sufficiently accurate and repeatable to provide useful information for long-term damage monitoring and post earth quake inspection.

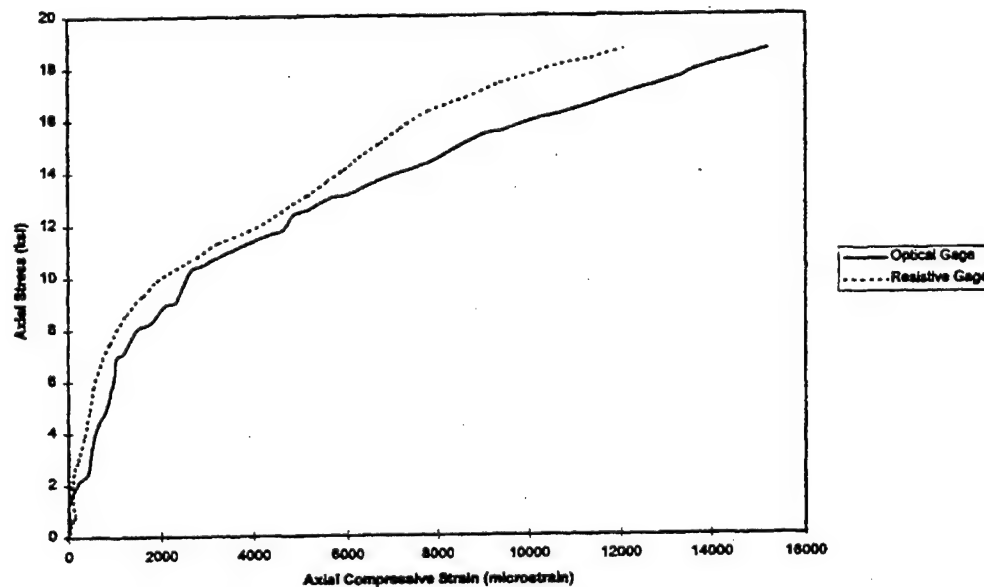


**Figure 3-26** Comparison of axial strain gage results from concrete cylinders  
(McCollum and Slattery, 1998)

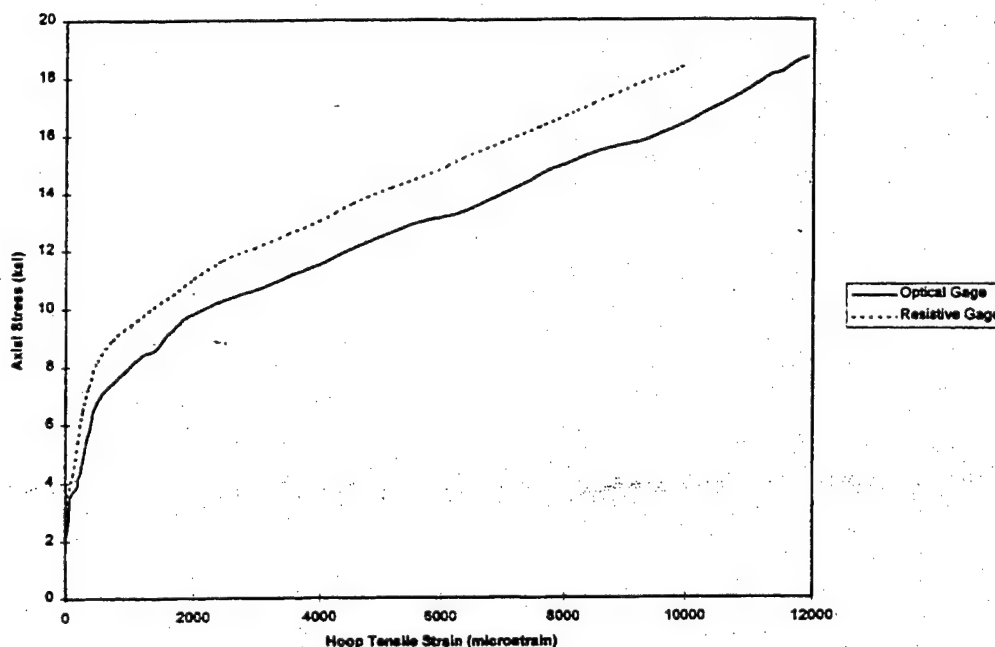


**Figure 3-27** Comparison of hoop strain gage results from concrete cylinders  
(McCollum and Slattery, 1998)

### 3.4 Chemical Sensor

As described earlier in section 3.0, Meltz, et al. (1991) had investigated a new fiber optic method for quasi-distributed remote chemical sensing. The tapped Bragg grating was developed as the foundation for the chemical sensor. Tapped Bragg grating sensors allow light to be tapped from the core of the fiber for various sensing purposes. In this case, Meltz et al. used the tap to provide light for excitation and to collect fluorescence from potential specific chemical species. [A schematic of the fiber Bragg grating tap was illustrated earlier in Figure 2-7]. The multipoint fiber Bragg grating chemical sensor used by Meltz et al. is schematically shown in Figure 3-28. Detailed calculations and modeling were carried out to determine the fraction of excitation light absorbed in the fluorescent layer of the sensor, and the collection efficiency of the tap from both single and multimode fiber Bragg rating chemical sensors. Meltz et al. concluded that power levels of at least a microwatt would be needed to obtain rapid response times and to resolve small concentrations. High power diode lasers are expected to be the preferred light source for a potential chemical sensor.

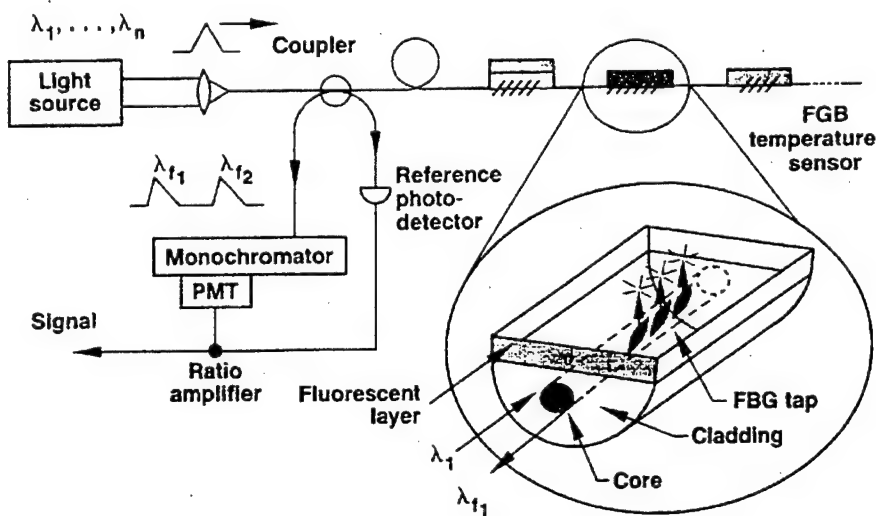


**Figure 3-28** Schematic of a multi-point fiber Bragg grating chemical sensor system  
(Meltz et al, 1991)

### 3.5 Corrosion

The investigation of a tapped Bragg grating corrosion monitoring sensor concept for use on military aircraft was reported by Perez et al. (1995a). A potential sensing system was designed where the tapped light is absorbed by a chemical species with an absorption spectrum that is sensitive to iron ion concentration. The basic equations needed to design a tapped Bragg grating corrosion sensor were derived and a summary provided of the derivation. [The derivation was fully developed and published in its entirety in Perez, et al. (1995b) and discussed previously in Section 2.0]. Perez et al. concluded that the spectral width for the tapped Bragg gratings was orders of magnitude larger than for the

case of a Bragg grating. This fact considerably limits the number of sensors, as compared to the large numbers of Bragg gratings that can be placed in a single optical fiber without cross coupling.

A potential concept for a tapped Bragg grating corrosion sensor was developed based on a electrochemical species that responds to changes in the environment surrounding the sensor that result from the corrosion process itself (Perez et al. 1995a). Ferroin (1,10 Phenanthroline) was chosen as the indicator species that would respond to the presence of iron ions from the oxidation or corrosion process of iron and steels. Figure 3-29 shows the transmission absorption spectra of Ferroin as a function of the concentration of iron ions. Small amounts of iron ions in this solution can substantially increase the absorption behavior. Perez et al. concluded that this behavior would provide a potential concept for a tapped Bragg grating corrosion sensor. They envision a tapped Bragg grating coated with this type of buffer layer surrounded by a non-continuous metallic reflector to collect back the tapped radiation as shown in Figure 3-30. The amount of corrosion would be proportional to the decrease in intensity.

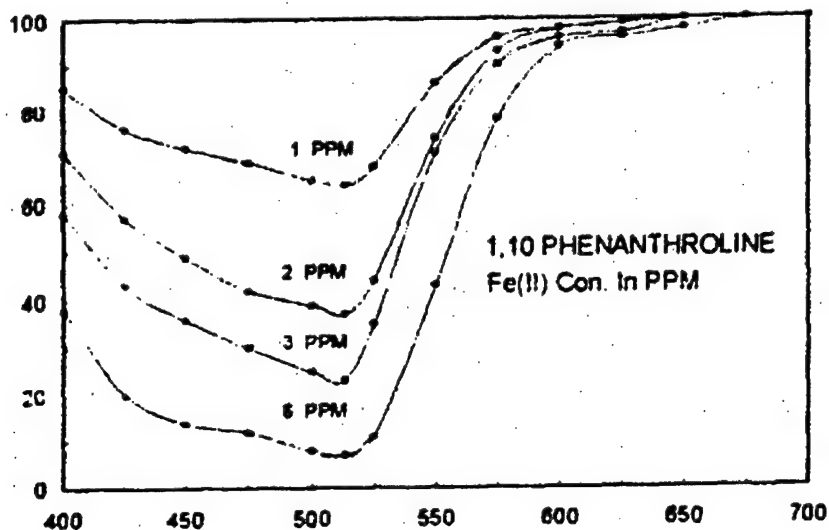


**Figure 3-29** Absorption spectral of Ferroin  
(Perez et al, 1995)

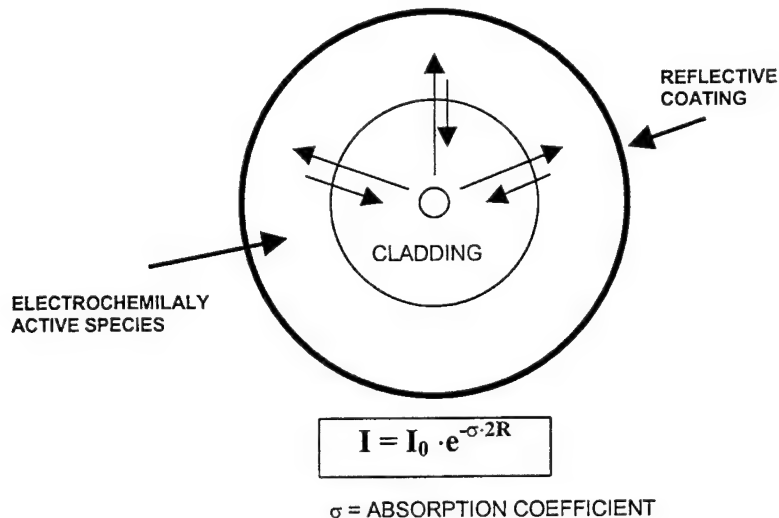


**Figure 3-30** Potential concept for a Tapped Bragg Grating corrosion sensor  
(Perez et al, 1995)

### 3.6 Adhesive Joints

Shultz et al. (1999, 2000) reported on research to develop health monitoring of an adhesive joint using a multi-axis fiber grating strain sensor. This research topic was chosen because the use of adhesive joints in aerospace structures is becoming increasingly important, and there is a need for assessing joint integrity quickly, non-intrusively, accurately, and inexpensively. Schulz et al. used multi-axis strain sensors developed by Udd et al. (1998, 2000). These sensors are formed from dual overlaid gratings written onto polarization preserving fiber as shown in Figure 3-31. The sensors were coated with polyimide and have a diameter of 135 micrometers. When a broadband light source is used, four spectral peaks are reflected (one peak for each grating and polarization axis). Axial strain is measured from the wavelength peak shift and transverse strain is measured from the peak to peak separation. Figure 3-32 shows the response of the multi-axis fiber grating sensor to axial and transverse strains. Schulz et al. instrumented aluminum double lap adhesive joints with multi-axis sensors embedded into the joint. Figure 3-33 shows the type of specimens used and the three different sensor orientations used in the study. The orientations were 45, 90, and 135 degrees from the loading direction. Retrofitting of sensors to existing joints as shown Figure 3-34 was also studied.

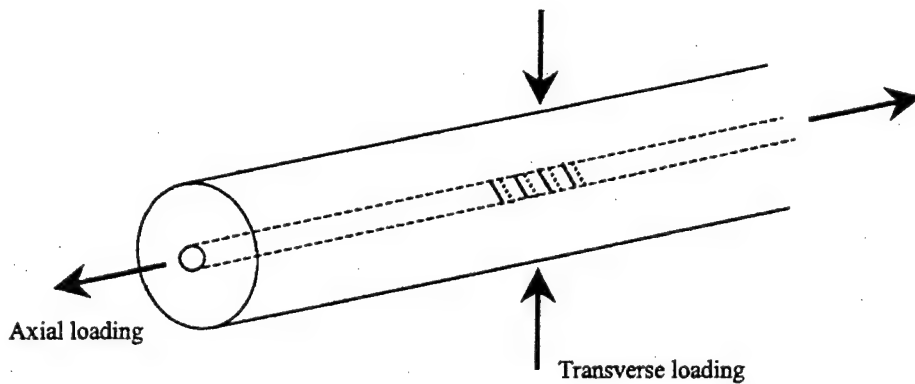


**Figure 3-31** Axial and transverse load sensing directions of multi-axis fiber grating strain sensor  
(Schulz et al, 2000)

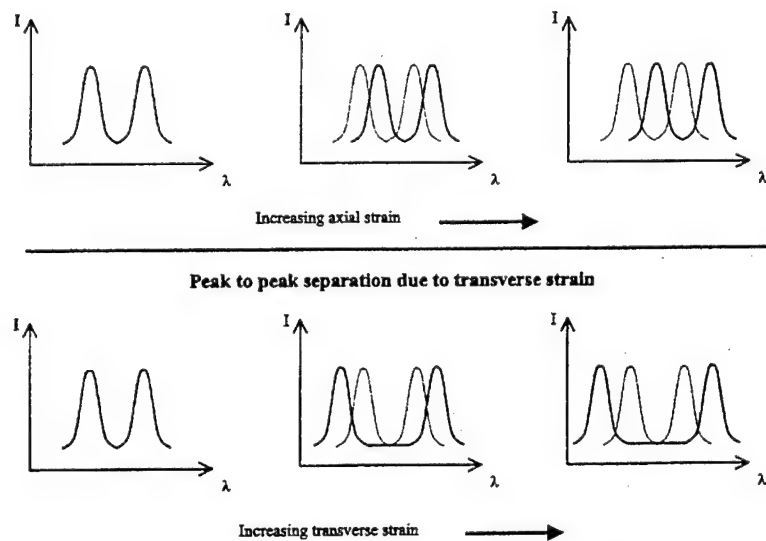


**Figure 3-32** Response of multi-axis fiber grating strain sensor to axial and transverse strains  
(Schulz et al, 1999)

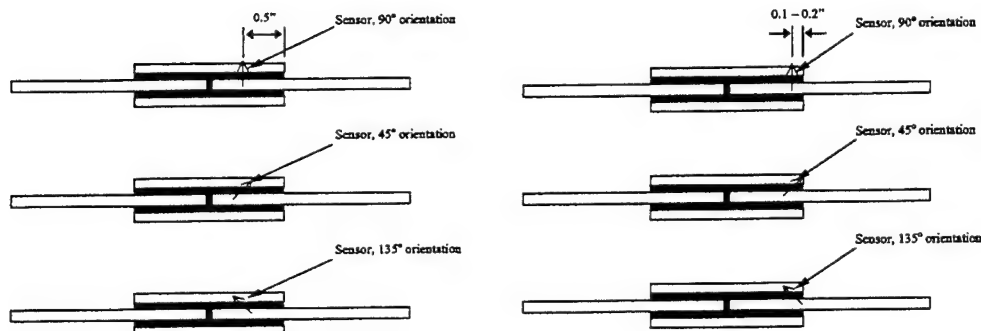


**Figure 3-33** Multi-axis strain sensors embedded into inner (left) and edge (right) locations of adhesive bond with different orientations  
(Schulz et al, 1995)

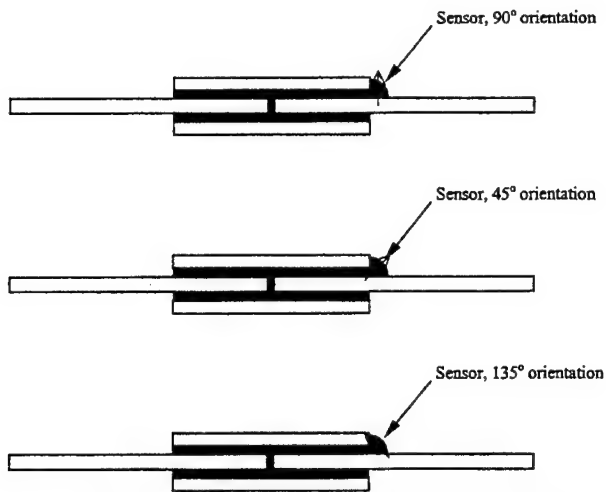
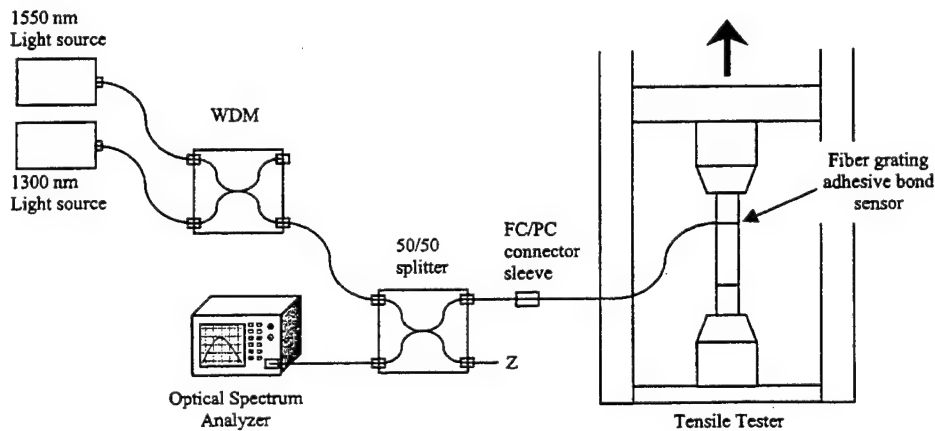


Figure 8. Retrofit of multiaxis sensor to existing adhesive joint

**Figure 3-34** Retrofit of multi-axis sensor to existing adhesive joint  
(Schulz et al, 1999)

The testing system used for instrumented adhesive joints is shown in Figure 3-35 (Shultz 1999, 2000). An optical spectrum analyzer was used to obtain the spectra from the sensors. Two broadband edge light emitting diode light sources were used to obtain the four reflected spectral peaks from the sensor. Schulz et al. carried out tensile testing and fatigue testing on the lap joint samples and provided data and analysis of the results. It was concluded that multi-axis fiber grating sensors embedded in adhesive joints could measure shear strain when the transverse sensing axes are aligned with the shear direction. The embedded sensors also could be used to identify the state of the part and predict joint failure. The embedded sensors were robust and did not significantly reduce joint strength. In addition, the retrofitted sensors provided strain information.



**Figure 3-35** Loading and demodulation setup during tensile testing of instrumented adhesive joints  
(Schulz et al, 1999)

### 3.7 Acoustic Emission and Ultrasonic Waves

In a recent study, Perez, et al. (2001) investigated the use of fiber optic Bragg grating sensors to detect acoustic emission signals. The authors were motivated to carryout this study because of the need to develop easily embedded acoustic emission sensors for health monitoring. Acoustic emission sensors are used to detect the acoustic energy in the form of ultrasonic waves emanating from crack initiation and propagation in structures. The advantage of Bragg grating fiber optic sensors is that as contrasted to piezoelectric ultrasonic sensors, they are easily embedded in or mounted on the surface of structures. In addition, Bragg grating sensors are ideal for multiple sensor applications and can be employed in parallel or in series using wavelength division or time division methods. Perez et al. believe it is reasonable to envision hundreds of fiber Bragg grating sensors embedded in an airplane wing for health monitoring. Perez et al. point out the challenges that needed to be addressed to make this health monitoring system a reality. First the detection sensitivity must be very high. Second, detection speed must be high enough to capture instantaneously most of the frequency content of the acoustic emission signal. Third, a sophisticated computer-based real-time data acquisition, processing and analysis system must developed.

Perez et al. established the sensitivity and speed of fiber Bragg grating sensors by performing a series of experiments with the sensors using controlled generation of ultrasonic signals. Figure 3-36 shows a schematic of the experimental setup. The fiber Bragg grating sensors were glued to the surface of the acoustic resonator, so that the resonator is set into vibration in its thickness-extension mode. This causes the fiber grating to be stretched and shortened periodically at the frequency of the acoustic resonator. A super-radiant luminescent light source is used to send light (centered at 1300 nm, with a spectral width of 30 nm, and peak power of 1.3 mW) down the fiber. A high-speed photodetector is used to convert the light signal to an electrical signal for display on an oscilloscope. Since the PZT resonators have frequencies ranging from 20 kHz to 2 MHz, Perez et al. were able to investigate the response of the Bragg grating sensors to acoustic emission signals over a wide range. Figure 3-37 shows a typical waveform of the acoustic signal, the trigger, and the response, at a frequency of 355 kHz. Several Bragg grating sensors were tested at a variety of frequencies. Perez et al. concluded that they had obtained very promising experimental evidence that fiber Bragg grating sensors may be used to detect acoustic emission events. This detection method is very sensitive and approaches the currently available methods of acoustic emission detection. The method is also highly reliable, and can be easily adapted to structural monitoring.

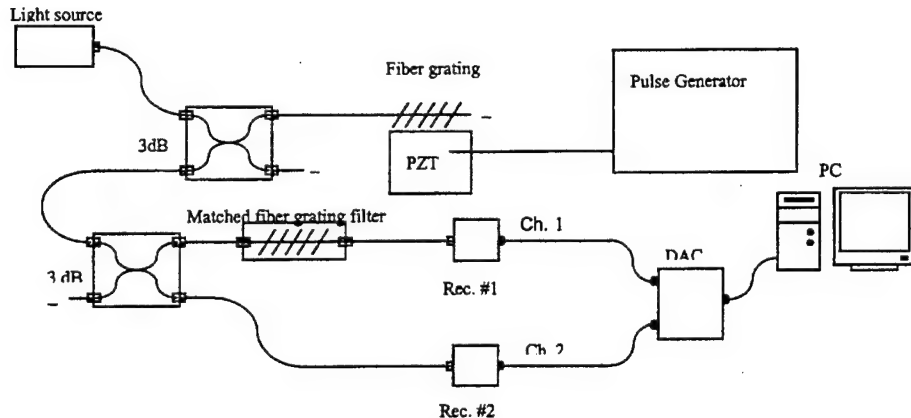


**Figure 3-36** Block diagram of the experimental setup for characterizing Bragg grating sensors  
 (Perez et al, to be published)

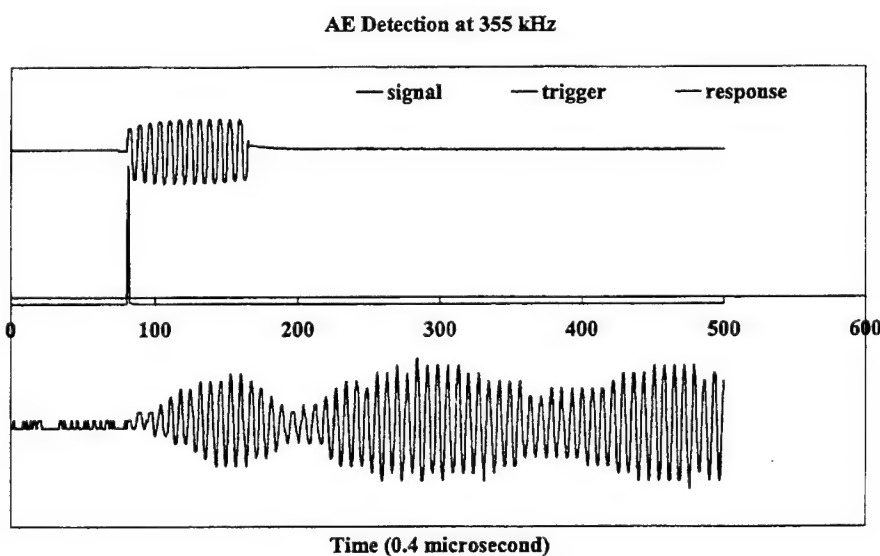


**Figure 3-37** Pulse acoustic signal, trigger, and response at 355 kHz  
 (Perez et al, to be published)

In another study, Perez, et al. (2000) report on improving the sensitivity of fiber Bragg grating sensors to high frequency ultrasonic waves (acoustic emission) and on obtaining a theoretical understanding of the problem. The experimental efforts focus on determining the effects of the Bragg grating length to ultrasound-wavelength ratio on the detection sensitivity. Fiber Bragg grating sensors, 1 mm, 2 mm, 4 mm, and 6 mm long, were bonded to piezoelectric crystals of comparable thickness. A large number of frequencies ranging from 10 kHz to 2 MHz were used to determine the effect of frequency on system sensitivity. The same experimental system shown earlier in Figure 3-36 was used where a matched Bragg grating was used in the demodulation side of the detection system to enhance detection sensitivity. Figure 3-38 shows the response of the fiber Bragg grating sensors to (simulated) acoustic emission signals as a function of frequency.

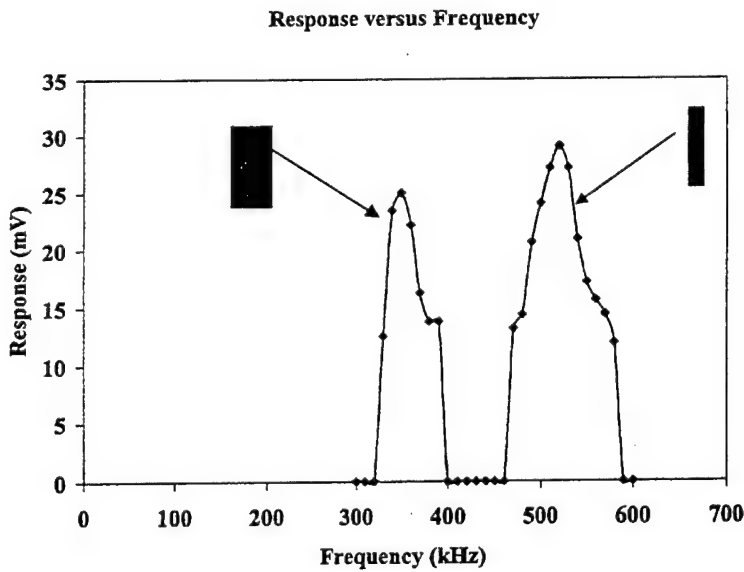


**Figure 3-38** Response of fiber Bragg grating sensor to acoustic emission as a function of frequencies  
 (Perez et al, 2000)

Perez et al. also theoretically modeled the problem of the coupling of an ultrasonic wave to light waves propagating through a fiber Bragg grating sensor. An approach based on coupled wave theory commonly used in propagation and scattering of electromagnetic waves was used. Figure 3-39 shows a schematic of the model. Perez et al. concluded that fiber Bragg gratings could detect a minimum displacement of about  $2 \times 10^{-11}$  m. At 2 MHz, the minimum detectable strain was about 0.02 micro strains. This sensitivity is approaching the currently available methods of acoustic emission detection. Perez et al. believe that a tunable demodulating fiber grating will enhance sensitivity and they are in the process of employing a stretching apparatus to achieve the improved sensitivity.

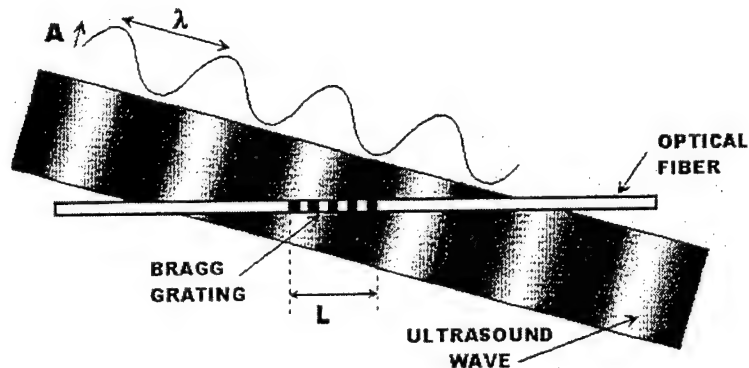


**Figure 3-39** Schematics of interaction of ultrasound wave with light wave going through a fiber Bragg grating  
 (Perez et al, 2000)

## **4.0 CONCLUSIONS AND PROGNOSIS**

### **4.1 Conclusions and Summary**

Fiber optic Bragg grating sensors coupled with a variety of demodulation or readout techniques offer an elegant means to monitor the processing or health of materials in a variety of applications. Laboratory research has demonstrated the feasibility of using fiber optic Bragg grating sensors to determine strain and temperature in structures, monitor the processing of composites, monitor adhesive joints, serve as chemical sensors and corrosion detection sensors, and to detect acoustic emission. Several multiplexing techniques have been demonstrated that allow a number of sensors to be used on a single fiber.

The seminal research on fiber optic Bragg gratings was carried out over twenty years ago, and research on fiber Bragg grating sensors has been active for about fifteen years. However, designers and the NDE community are apparently not very aware of the technology, and have not used the full promise of fiber optic Bragg grating sensors in actual field applications.

Research on fiber optic Bragg gratings was reported in a watershed paper in 1978 by Hill et al. The authors were motivated by optical communications applications, and developed the first photoinduced in-fiber Bragg gratings. In 1987, Meltz, et al. made an important advance in Bragg grating technology when they showed that in-fiber Bragg gratings can be formed by illuminating the fiber core from the side with coherent UV radiation. This side writing technique expanded the range and choice of the Bragg period or spacing. In the 1990s, research continued on optical fiber Bragg gratings. Morey, et al. (1991) first demonstrated a multiplexing technique for placing and interrogating a number of Bragg gratings along the same fiber. Also, Meltz, et al. (1991) developed the tapped Bragg grating sensor and showed that light could be tapped from a fiber and used for a chemical sensor. The light tapped out of the fiber was used to excite the fluorescence of a chemical species that was in the vicinity of the fiber, and in turn the light would then reenter the tap and be analyzed by the sensor. This same technology was latter used Perez, et al. (1995a) to demonstrate a fiber Bragg grating corrosion detection sensor. Perez, et al. (1995b) also developed a physical and mathematical model to improve understanding and design of tapped Bragg gratings.

Hill, et al. (1993) demonstrated a new methodology for fabricating fiber optic Bragg gratings by exposing monomode photosensitive fiber to UV radiation through a phase mask. Under computer control, this approach offered low- cost devices, and great flexibility for varying the pitch and the strength of the Bragg grating coupling coefficients. Askins, et al. (1995) developed a new in-line technique for rapidly and inexpensively making fiber Bragg ratings as the fiber is drawn in the production process. By using a computer controlled interferometer Askins and coworkers could also write an array of Bragg gratings with varying wavelength for multiplexing.

There has been a wide array of applications demonstrated for Bragg grating sensors. In early work (Meltz 1987) strain and temperature measurements were demonstrated with a fiber Bragg grating sensors in composite materials. Kersey and T. A. Berkoff (1992) followed this by a report on their research on a fiber optic differential temperature sensor. Measures, et al. (1992) developed a wavelength demodulation Bragg grating fiber optic sensing system for measuring strain in smart structures. A number of other researchers reported of various advances in the demodulation techniques and in further applications.

Research on applications continued with fiber Bragg gratings being used to monitor composite processing by Lawrence, et al. (1996), Slattery, et al. (1998), and Kalamkarov et al. (1998). A large number of researchers also reported results of monitoring civil structures with fiber Bragg grating sensors. For example, Maher, et al. (1993) Chen, et al. (1994), Navy (1995), and Davis et al. (1996). The research even progressed to research on monitoring a full-scale laboratory bridge by Kodiindouma, et al. (1996). Research on Bragg grating chemical sensors and corrosion detection sensors was mentioned earlier in the summary. Research has also been reported on monitoring of adhesive joints by Shultz et al, (1999) and on detection of acoustic emission by Perez et al. (2000).

## 4.2 Prognosis/Recommendations

Laboratory research has demonstrated the feasibility of using fiber optic sensors in a variety of applications, but the insertion of this technology into existing and new field applications has been slow to evolve. In order to help with insertion, a workshop on fiber Bragg grating sensors for designers and NDE engineers is recommended. In addition, federal funding agencies should consider expanding their sponsorship of full field demonstrations of fiber Bragg grating sensors in several different existing and new field applications. Research needs to continue on improving the robustness and ease of use of the total systems including the demodulation or readout devices. Researchers should consider expanding publication of results in materials and NDE journals and periodicals as contrasted to the past publications that have been heavily focused on instrumentation and optical journals. In the end, the elegant and exquisitely sensitive fiber Bragg gratings will find wide spread use, first in high value added applications and then in more common applications.

## REFERENCES

- Askins, C. G., M. A. Putnam, G. M. Williams, E. J. Friebel, "Stepped-wavelength optical-fiber Bragg grating arrays fabricated in line on a draw tower," *Optical Society of America, Optics Letters*, Volume 19, No. 2, January, 1994, pp. 147 – 149.
- Bhatia, V., T. D'Alberto, K. A. Murphy, R. O. Claus, C. P. Nemarich, "Comparison of Optical Fiber Long-Period and Bragg Grating Sensors," *SPIE*, Volume 2093, 1996, pp. 110 – 121.
- Chen, B., M. H. Maher, E. G. Nawy, "Fiber-Optic Bragg Grating Sensor for Nondestructive Evaluation of Composite Beams," *Journal of Structural Engineering*, Volume 120, No. 12, December, 1994, pp. 3456 – 3470.
- Davis, M. A., A. D. Kersey, "All-fiber Bragg grating sensor demodulation technique using a wavelength division coupler," *IEEE, Electronics Letters Online*, No. 19940059, November, 1, 1993, 3 pp.
- Davis, M. A., D. G. Bellemore, T. A. Berkoff, A. D. Kersey, M. A. Putnam, R. L. Idriss, M. Kodinduma, "Fiber Optic Sensor System for Bridge Monitoring with Both Static Load and Dynamic Modal Sensing Capabilities," *SPIE*, Volume 2946, 1996, pp. 219 – 232.
- De Paula, R. P., J. W. Berthold III, "Fiber Optic and Laser Sensors XIV," *SPIE*, Volume 2839, August, 1996, pp. 63 – 75.
- Hill, K. O., B. Malo, F. Biladeau, D. C. Johnson, J. Albert, "Bragg gratings fabricated in a monomode photosensitive optical fiber by UV exposure through a phase mask," *Appl. Phys. Lett.*, Volume 62, No. 10, March, 1993, pp. 1035 – 1037.
- Hill, K. O., Y. Fujii, D. C. Johnson, B. S. Kawasaki, "Photosensitivity in optical wave guides: Application to reflection filter fabrication," *Appl. Phys. Lett.*, Volume 32, No. 10, May, 1978, pp. 647 – 649.
- Jones, R. T., T. A. Berkoff, D. G. Bellemore, D. A. Early, J. S. Sirkis, M. A. Putnam, E. J. Friebel, A. D. Kersey, "Cantilever Plate Deformation Monitoring Using Wavelength Division Multiplexed Fiber Bragg Grating Sensors," *SPIE*, Volume 2093, 1996, pp. 258 – 268.
- Kalamkarov, A. L., S. B. Fitzgerald, D. O. MacDonald, A. V. Georgiades, "Smart pultruded composite reinforcements incorporating fiber optic sensors," *SPIE*, Volume 3400, 1998, pp. 94 – 105.
- Kersey, A. D., T. A. Berkoff, "Fiber-Optic Bragg-Grating Differential-Temperature Sensor," *IEEE Photonics Technology Letters*, Volume 4, No. 10, October, 1992, pp. 1183 – 1185.

- Kodindouma, M. B., R. L. Idriss, A. D. Kersey, M. A. Davis, D. G. Bellemore, E. J. Friebel, M. A. Putnam, "Damage Assessment of a Full Scale Bridge Using an Optical Fiber Monitoring System," *SPIE*, Volume 2719, 1996, pp. 265 – 275.
- Lambelet, P., P. Y. Fonjallaz, H. G. Limberger, R. P. Salathe, Ch. Zimmer, H. H. Gilgen, "Bragg Grating Characterization by Optical Low-Coherence Reflectometry," *IEEE Phototonics Technology Letters*, Volume 5, No. 5, May, 1993, pp. 565 – 567.
- Lawrence, C. M., D. V. Nelson, J. R. Spingarn, T. E. Bennett, "Measurement of Process-Induced Strains in Composite Materials Using Embedded Fiber optic Sensors," *SPIE*, Volume 2093, 1996, pp. 60 – 68.
- Maher, M. H., B. Chen, J. D. Prohaska, E. G. Nawy, E. Snitzer, "Non-Destructive Evaluation of Strain in Pre-stressed Concrete Structural Elements Using a Novel Fiber Optic Technology," *Proceedings of International Conference on NDT of Concrete in the Infrastructure*, June, 1993, pp. 467 – 476.
- McCollum, S. W., K. T. Slattery, "Structural damage monitoring in composite-confined concrete columns using Bragg gratings," *SPIE*, Volume 3396, 1998, pp. 14 – 21.
- Melle, S. M., A. T. Alvie, S. Karr, T. Coroy, K. Liu, R. M. Measures, "A Bragg Grating-Tuned Fiber Laser Strain Sensor System," *IEEE Photonics Technology Letters*, Volume 5, No. 2, February, 1993, pp. 263 – 266.
- Meltz, G., J. R. Dunphy, W. H. Glenn, J. D. Farina, F. J. Leonberger, "Fiber optic temperature and strain sensors," *SPIE*, Volume 798, 1987, pp. 104 – 114.
- Meltz, G., W. W. Morey, J. R. Dunphy, "Fiber Bragg Grating Chemical Sensor," *SPIE*, Volume 1587, 1991, pp. 350 – 361.
- Meltz, G., W. W. Morey, W. H. Glenn, "Formation of Bragg gratings in optical fibers by a transverse holographic method," *Optical Society of America, Optic Letters*, Volume 14, No. 15, August 1, 1989, pp. 823 – 825.
- Morey, W. W., J. R. Dunphy, G. Meltz, "Multiplexing fiber Bragg grating sensors," *SPIE*, Volume 1586, 1991, pp. 216 – 224.
- Nawy, E. G., "Use of Fiber Optic Sensors for the Non-Destructive Strength Evaluation and Early Warning of Impending Failure in Structural Components," *Research Transformed into Practice: Implementation of NSF Research*, 1995, pp. 210 – 220.
- Nawy, E. G., B. Chen, "Bragg Grating Fiber Optic Sensing the Structural Behavior of Continuous Composite Concrete Beams Reinforced with Pre-stressed Prisms," *Proceedings of 2<sup>nd</sup> International Conference on NDT of Concrete in the Infrastructure*, June, 1996, pp. 1 – 10.

Parriaux, O., E.-B. Kley, B. Culshaw, M. Breidne, "Micro-optical Technologies for Measurement, Sensors, and Microsystems II and Optical Fiber Sensor Technologies and Applications," *SPIE*, Europe Series, Volume 3099, June, 1997, pp. 316 – 326.

Perez, I. M., H. L. Cui, E. Udd, "A Fiber Bragg Grating Sensor for Acoustic Wave Emission," *to be published*, pp. 1 – 4.

Perez, I. M., H. L. Cui, E. Udd, "High Frequency Ultrasonic Wave Detection Using Fiber Bragg Gratings," *(to be published) SPIE Smart Structures Conference*, Newport Beach, March, 2000.

Perez, I., T. Bibby, M. Ryan, "Fiber Optic Bragg Grating Model," *Final Report, NAWCAWAR-95027-4.3*, Naval Air Warfare Center, Aircraft Division Warminster, P. O. 5152, Warminster, PA. 18974-0591, 24 pp.

Perez, I., V. Agarwala, R. Scott, S. D. Tyagi, "Bragg Grating Corrosion Sensor," *Review of Progress in Quantitative Nondestructive Evaluation*, Volume 14, 1995, pp. 2081 – 2088.

Perez, I., V. Agarwala, W. R. Scott, S. D. Tyagi, "Bragg Grating Corrosion Sensor," *Review of Progress in QNDE*, Volume 14, pp. 2081 – 2088.

Schulz, W. L., E. Udd, J. M. Seim, I. Perez, A. Trego, "Progress on monitoring of adhesive joints using multi-axis fiber grating sensors," *(to be published) SPIE Smart Structures Conference*, Newport Beach, March, 2000, 10 pp.

Schulz, W. L., E. Udd, M. Morrell, J. Seim, I. Perez, A. Trego, "Health monitoring of an adhesive joint using a multi-axis fiber grating strain sensor system," *SPIE*, Volume 3586, 1999, pp. 41 – 52.

Sennhauser, U., A. Frank, P. Mauron, Ph. M. Nellen, "Reliability of Optical Fiber Bragg Grating Sensors at Elevated Temperature," *IEEE, 38<sup>TH</sup> Annual International Reliability Physics Symposium*, San Jose, California, 2000, pp. 264 – 269.

Sennhauser, Urs, Rolf Bronnimann, and Phillip M. Nellen, "Reliability Modeling and Testing of Optical Fiber Bragg Sensors for Strain Measurements," *SPIE*, Vol. 2839, 1996, pp. 64-75.

Sennhauser, Urs, Rolf Bronnimann, Pascal Mauron, and Philipp M. Nellen, "Reliability and Durability of Fiber Grating Sensors in Structural Monitoring Applications," *SPIE*, Vol. 3099, 1997, pp. 317-326.

Slattery, K. T., K. Corona-Bittick, D. J. Dorr, "Composite cure monitoring with Bragg grating sensors," *SPIE*, Volume 3399, 1998, pp. 114 – 121.



## BIBLIOGRAPHY

Davis, M. A., D. G. Bellemore, A. D. Kersey, M. A. Putnam, E. J. Friebel, R. L. Idriss, M. Kodinduma, "High Sensor-Count Bragg Grating Instrumentation System for Large-Scale Structural Monitoring Applications," *SPIE*, Volume 2718, 1996, pp. 303 – 309.

Davis, M. A., A. D. Kersey, "Separating the Temperature and Strain Effects on Fiber Bragg Grating Sensors Using Stimulated Brillouin Scattering," *SPIE*, Volume 2093, 1996, pp. 270 – 278.

Elster, J., J.A. Greene, M. E Jones, T.A. Bailey, I. Perez, "Optical Fiber Corrosion Sensors for Aging Aircraft," *SPIE*, Vol. 3399, Process Control and Sensors for Manufacturing, March, 1998, pp. 28-33.

Elster, J., J. Greene, M.E. Jones, T.A. Bailey, S.M. Lenahan, and I. Perez, "Optical Fiber-Based Corrosion Sensors for Aging Aircraft," *The Second Joint NASA/FAA/DoD Conference on Aiding Aircraft*, Aug 31, 1998.

Elster, J., J. Greene, M. Jones, T. Bailey, S. Lenahan, W. Velander, R. VanTassell, W. Hodges, and I. Perez. "Optical Fiber-Based Chemical Sensors for Detection of Corrosion Precursors and By-Products," *SPIE International Symposium on Industrial and Environmental Monitors and Biosensors in Boston*, Massachusetts, November 2-5<sup>th</sup>, 1998.

Elster, Jennifer L. Elster, Jonathan A. Greene, Mark E. Jones, Tim A. Bailey, Shannon M. Lenahan, and Ignacio M. Perez, "Optical Fiber-Based Corrosion Sensors for Aging Aircraft," *The Second Joint NASA/FAA/DoD Conference on Aging Aircraft*, Williamsburg, VA, Aug 1998.

Elster, Jennifer, Jonathan Greene, Mark Jones, Tim Bailey, Shannon Lenahan, William Velander, Roger VanTassell, William Hodges, and Ignacio M. Perez, "Optical Fiber-Based Chemical Sensors for Detection of Corrosion Precursors and By-Products," *SPIE Industrial and Environmental Monitors and Biosensors*, Boston, November, 1998.

Elster, Jennifer L., Mark E. Jones, William Velander, and Ignacio M. Perez, "Optical Fiber-Based Corrosion Monitoring Systems," *NDE Session 3: Systems Health Monitoring*, presentation N3.4, Aeromat '99 Conference, Dayton, OH, June, 1999.

Elster, Jennifer L., Mark E. Jones, Kent A. Murphy, Mike F. Gunther, Ignacio M. Perez, Stephen Doherty, and Rudi Seitz, "Optical Fiber-Based Chemical Sensors Using Microsphere Coated Long Period Gratings,"

Greene, Jonathan A., Mark E. Jones, Tim A Bailey, Ignacio M. Perez, "Optical Fiber Corrosion Sensors for Aging Aircraft," *SPIE*, Volume. 3399, Process Control and Sensors for Manufacturing, March, 1998, San Antonio, TX, pp. 28-33.

Jones, Mark E., Jennifer L. Elster, William Velander, and Ignacio M. Perez, "Optical Fiber-Based Corrosion Monitoring Systems," MRS Conference, Cincinnati, OH, Nov 1999.

Kersey, A. D., M. A. Davis, D. Bellemore, "Development of Fiber Sensors For Structural Monitoring," *SPIE*, Volume 1809, 1995, pp. 262 – 268.